Environmental and economic assessment of transportation fuels from municipal solid waste

by

Pooja Suresh

B.Eng. Aerospace Engineering
Carleton University, 2012

SUBMITTED TO THE DEPARTMENT OF AERONAUTICS AND ASTRONAUTICS IN PARTIAL FULFILLMENT OF THE REQUIREMENTS FOR THE DEGREE OF

MASTER OF SCIENCE IN AERONAUTICS AND ASTRONAUTICS
AT THE
MASSACHUSETTS INSTITUTE OF TECHNOLOGY

JUNE 2016

Signature of Author.....
Department of Aeronautics and Astronautics
May 19, 2016

Certified by.....
Steven R.H. Barrett
Associate Professor of Aeronautics and Astronautics
Thesis Supervisor

Accepted by.....
Paulo C. Lozano
Associate Professor of Aeronautics and Astronautics
Chair, Graduate Program Committee

Environmental and economic assessment of transportation fuels from municipal solid waste

by

Pooja Suresh

Submitted to the Department of Aeronautics and Astronautics
on May 19, 2016 in Partial Fulfillment of the
Requirements for the Degree of Master of Science in
Aeronautics and Astronautics

ABSTRACT

Municipal solid waste (MSW), comprising food waste, residential rubbish and commercial waste, has been identified as a potential feedstock for the production of alternative fuels. Conversion of MSW to fuel could displace petroleum-derived fuels to mitigate greenhouse gas (GHG) emissions from transportation, and also avoid the GHG emissions associated with existing waste management strategies such as landfilling. This thesis quantifies the lifecycle GHG emissions and economic feasibility of middle distillate (MD) fuel, including diesel and jet fuel, derived from MSW in the United States via three thermochemical conversion pathways: conventional gasification and Fischer-Tropsch (FT MD), plasma gasification and Fischer-Tropsch (Plasma FT MD) and, conventional gasification, catalytic alcohol synthesis and alcohol-to-jet upgrading (ATJ MD). Expanded system boundaries are used to capture the change in existing MSW use and disposal, and parameter uncertainty is accounted for with Monte Carlo simulations.

The median lifecycle GHG emissions are calculated to be 32.9, 62.3 and 52.7 gCO_2e/MJ with standard deviations of 7.2, 9.5 and 13.2 gCO_2e/MJ for FT, Plasma FT and ATJ MD fuels, respectively, compared to a baseline of 90 gCO_2e/MJ for conventional MD fuels. These results are found to be sensitive to MSW composition, the waste management strategy displaced, plant scale and associated fuel yield, feedstock transportation distance and the co-product allocation method. Median minimum selling prices are estimated at 0.99, 1.78 and 1.20 $ per litre and standard deviations of 0.14, 0.29 and 0.27 $ per litre with the probability of achieving a positive net present value of fuel production at market prices of 14%, 0.1% and 7% for FT, Plasma FT and ATJ MD fuels, respectively. The sensitivity of these results to the discount rate, income tax rate, implementation of carbon price, feedstock cost, scale and process efficiency indicate that policy measures, MSW tipping fees and technological advancements can improve the economic viability of MSW fuels. Considering a societal perspective (e.g. social opportunity cost of capital, social costs of GHG emissions) increases the probability of positive net present value of fuel production to 93%, 67% and 92.5% for the FT, Plasma FT, and ATJ MD fuels, respectively.

Thesis Supervisor: Steven R.H. Barrett
Title: Associate Professor of Aeronautics and Astronautics

Acknowledgements

I would first like to thank my advisors, Prof. Steven Barrett and Dr. Robert Malina for their guidance and support in making this work possible and for being inspiring mentors to me, encouraging and advising me both at MIT and for my future career. I am thankful to Robert for his expertise and intuition that have helped shape my research, for motivating me and for teaching me valuable lessons in diplomacy.

I would also like to thank the US Federal Aviation Administration for sponsoring this work. I am grateful to Damian Blazy at Oliver Wyman, Dr. James Hileman at the FAA, and Dr. Wallace Tyner and Xin Zhao at Purdue University for offering their time and guidance on technical matters.

I have had the pleasure of working with exceptional friends and colleagues at the Laboratory for Aviation and the Environment. I would like to specially thank Akshay Ashok, Mark Staples, Matthew Pearlson and Philip Wolfe for their advice and support towards my research, and Irene Dedoussi, Lawrence Wong and Luis Alvarez for all the wonderful experiences that I will remember MIT by.

Finally and most importantly, I am thankful to my parents, Lata and Suresh, my sister, Shalini and my fiancé, Andrew for their unconditional support and understanding. Thank you for being my harshest critics and loudest cheerleaders. Thank you Andrew for driving a hundred thousand miles over the last two years, you inspire me to never give up.

Contents

List of Figures

List of Tables

Chapter 1 Introduction

Transportation accounted for approximately 27% of total greenhouse gas (GHG) emissions in the United States (US) in 2013 [1], with fossil fuels constituting over 95% of the sector's primary energy consumption [2]. Alternative fuels offer the potential to reduce GHG emissions from transportation compared to petroleum-derived fuels and have received considerable attention from academia, industry and regulators. Diesel and jet fuel make up approximately 35% of US transportation's energy consumption, which is projected to increase to 44% in 2040 [3], and federal agencies in the US have put in place mandates and goals specific to alternative diesel and jet fuel. For example, 60% of the fuel production mandates of the Renewable Fuels Standard (RFS2) in 2022 could be met with alternative diesel and jet fuel production [4], and the Federal Aviation Administration (FAA) has a goal of 1 billion gallons of alternative jet fuel consumption by 2018 [5].

Contrary to traditional crop-based feedstocks, waste-based feedstocks for alternative fuel production do not require additional land and do not directly compete with food production. Municipal solid waste (MSW), in particular, could offer a significant environmental advantage because the conversion of MSW to fuels would not only displace petroleum-derived fuels, but also avoid the GHG emissions associated with existing waste management strategies. In 2013, 34% of the total generated MSW in the US was recycled and composted, while the remaining 150 million tonnes (metric tons) of MSW, comprising food waste, residential rubbish and commercial waste, were discarded [6]. 80% of the discards were transferred to landfills [6],

where waste of biogenic origin releases anthropogenic methane, thereby making landfills the third-largest anthropogenic source of methane emissions in the US [7].

Along with environmental advantages, the economics of using MSW as a feedstock are potentially favorable, as US municipalities generally pay to dispose MSW in landfills. Average landfill tipping fees in the US amounted to $55/tonne in 2013, having increased every year since 2004 [6]. Charging tipping or processing fees may translate to a negative feedstock cost or source of revenue for MSW-derived fuels.

Finally, in contrast to fuels from other waste streams such as waste fats and greases [8], MSW derived fuels could replace relatively large shares of petroleum-derived MD fuel supply, as the energy content of the US national MSW discards in 2013 is equivalent to approximately 70% of same year US jet fuel consumption and 20% of the same year US transportation demand for all middle distillate fuels [2, 6, 9].

This analysis evaluates three thermochemical pathways that convert MSW to middle distillate (MD), i.e. diesel and jet, fuel: conventional gasification and Fischer-Tropsch (FT MD), plasma gasification and Fischer-Tropsch (Plasma FT MD) and, conventional gasification, catalytic alcohol (ethanol) synthesis and alcohol-to-jet upgrading (ATJ MD). Figure 1-1 illustrates the major technologies in each of the conversion pathways. These technologies are suited to the heterogeneity of MSW and have attracted commercial interest in recent years. Private corporations engaged in commercialization of these thermochemical processes include Fulcrum Bioenergy Inc., Solena Group Corp., Alter NRG Corp., Enerkem Inc. and Byogy Renewables Inc.

Despite the potential advantages and commercial interest in MSW MD fuels, only two peer-reviewed studies have addressed components of environmental and/or economic feasibility

for a limited number of pathways. Pressley et al. modeled conventional gasification and Fischer-Tropsch (FT) of MSW to MD, and carried out a lifecycle assessment to quantify the global warming potential of the conversion process [10]. Niziolek et al. also studied the same pathway, as well as methanol synthesis and conversion to gasoline and distillate as an alternative to FT, optimizing the process topology to estimate lifecycle CO_2 emissions of the plant and the break-even oil price [11]. No peer-reviewed analysis exists to date on the MSW to Plasma FT MD and the MSW to ATJ MD pathways.

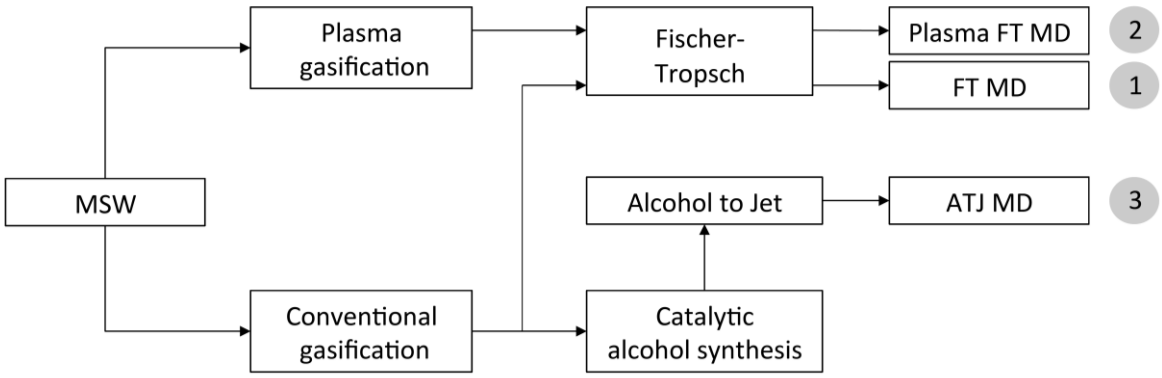

Figure 1-1: MSW to MD fuel pathways considered

Moreover, in contrast to previous studies, this thesis expands the system boundary to capture the change in the overall MSW lifecycle that results from using MSW to produce MD fuels rather than its existing use. Therefore, this work accounts for changes in GHG emissions and costs associated with the replacement of existing waste management strategies, additional recycling, end-of-life combustion and co-products.

Additionally, this thesis quantifies the uncertainty associated with the environmental and economic evaluation of these pathways. MSW-derived MD fuels have not yet been produced at a commercial scale owing to unresolved technical challenges, primarily the heterogeneity of the

feedstock, the lack of maturity of the conversion technologies resulting in low efficiency and yields, and high capital costs [9, 12]. Since no empirical data is available on the commercial performance of these technologies, the parameters in this analysis have large associated uncertainties. Moreover, costs and revenues occurring during future operation of the conversion plant are inherently uncertain. This analysis accounts for uncertainty in feedstock characteristics, technology performance and costs and revenues.

Though analyses of MSW MD fuels have been limited in the literature, lifecycle assessments (LCA) and techno-economic analyses (TEA) have been previously applied to thermochemical pathways that convert MSW to electricity and MSW to ethanol [13-18]. Moreover, a number of studies exist on thermochemical conversion of biomass to MD fuels [19-27]. The technology process models in these literature sources are referenced to estimate the material and energy balances associated with production of MSW MD fuels. Using US average MSW discards composition estimates [6], these balances are applied in conjunction with the US Environmental Protection Agency's (EPA) Waste Reduction Model (WARM) [28] and Argonne National Laboratory's Greenhouse Gases, Regulated Emissions, and Energy Use in Transportation (GREET) model [29], to calculate lifecycle GHG emissions.

The material and energy balances are also combined with historical market data, capital cost estimations and waste management industry heuristics in a discounted cash flow rate of return (DCFROR) model to calculate the minimum selling prices (MSP) of the fuels and net present value (NPV) of plant operation. Parameter uncertainty is captured using probability distributions and Monte Carlo simulations, and sensitivity analyses are used to assess the effect of variability of critical parameters. The results of this analysis provide information on the

potential of MSW MD fuels to reduce the GHG emissions intensity of transportation, their economic viability, and how these measures are affected by uncertainty and variability.

Chapter 2 Methods

2.1 System boundary

The analysis quantifies the change in GHG emissions and costs resulting from diverting MSW away from the prevailing waste management strategy to alternative MD fuel production [30, 31]. In this respect, it differs from other biomass-to-fuel LCA studies. MSW has a pre-existing lifecycle that is altered when it is used as fuel feedstock, whereas in the case of crop-based biomass, additional feedstock is cultivated for the purpose of fuel production. Therefore, this analysis excludes processes that occur irrespective of the waste management such as collection and existing sorting for recycling and composting. The system boundary does include the effects of eliminating waste management processes such as landfill, and accounts for the impacts of MSW conversion to MD fuels and their end-use.

The system boundary is shown in Figure 2-1. The system boundary is set where the MSW discards exit the sorting facility. Approximately 66% of the MSW generated in the US is discarded after the recycling and compost streams are separated out [6], and only these discards are included in this analysis. The US EPA's estimates of the composition of discarded MSW in the US in 2013 are used. The primary constituents are food waste (21.1%), plastics (17.7%), paper and paperboard (15.1%), rubber, leather and textiles (11.6%), metals (9.1%), yard trimmings (8.1%), wood (8%) and glass (5%) [6]. Future projections of MSW composition for

OECD countries show negligible change from the current empirical data, although the rate of MSW generation is expected to increase [32]. Therefore, the 2013 discards composition data from EPA is held constant throughout the analysis when future year projections are made for the TEA.

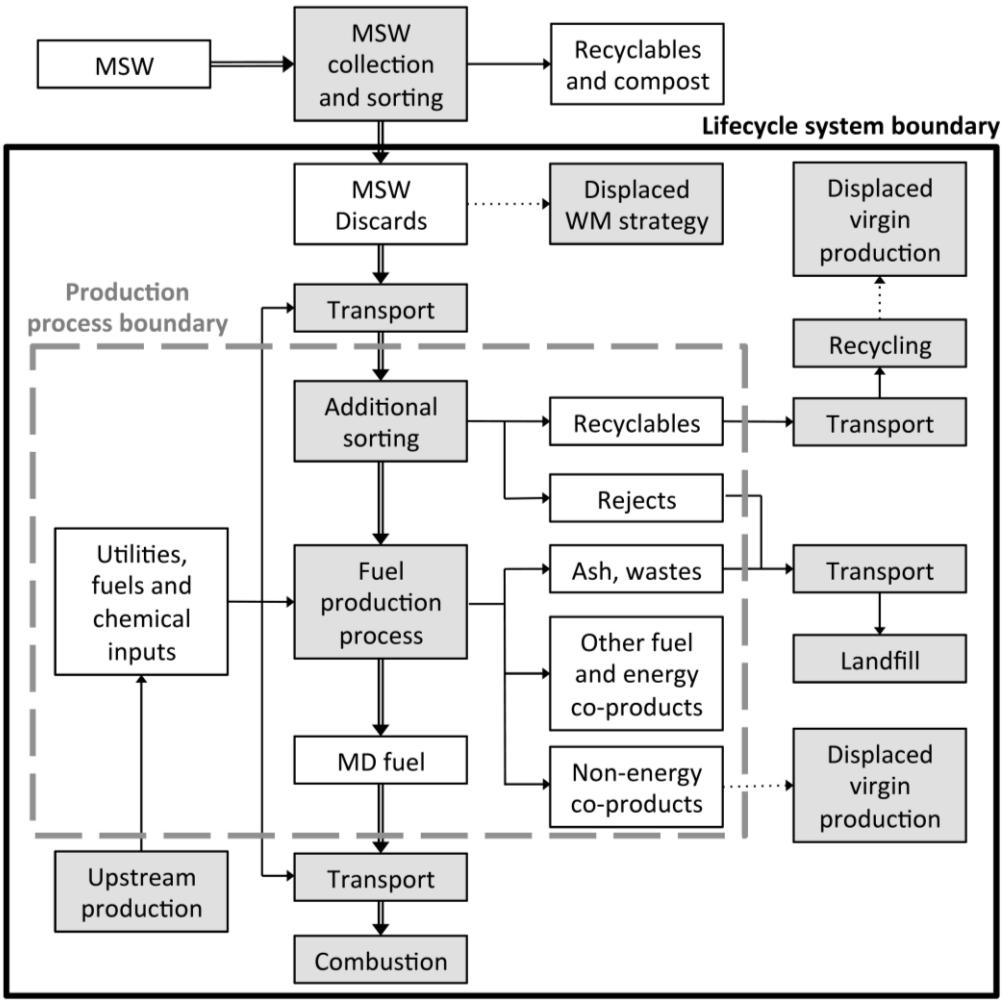

Figure 2-1: Expanded system boundary of the MSW to MD fuels lifecycle (solid line boundary) and fuel production process boundary (dashed line boundary). Double lined arrows indicate the primary material flow path. Single line arrows indicate secondary input and co-product material flows. Dotted line arrows connect to displaced processes. Processes are indicated with grey background.

The system boundary also includes the impact of displacing the existing management strategy for discards, which is a combination of landfill (approximately 80% of the discards) and incineration (the remainder) in the US [6]. The model accounts for transport of the feedstock to the fuel production plant. At the plant, further classification is required to adjust the feedstock composition in order to prevent contamination of equipment [11]. Non-combustibles such as metals, glass and other inorganics are sorted out, resulting in a higher heating value feedstock, which is then sized to meet the requirements of the gasifier. The pre-processing system is based on the Refuse Derived Fuel (RDF) facility model presented by Jones et al. [13] Major equipment includes conveyors, shredders, a magnetic separator for ferrous metals, an eddy current separator for aluminum, disc screens to sort by size, and air classification to sort the feedstock by weight. Assuming an average sorting efficiency of 90% [10], approximately 15% of the MSW feed is separated out during the pre-processing.

The recyclable scrap metals and glass removed from the feedstock are sold for recycling, and the rejects are sent to landfill. The GHG emissions impacts, revenues and costs associated with material recovery and disposal of rejects are included within the system boundary. The pre-processed feedstock is then directed to the fuel production process. The material, energy and carbon balances for the conversion technologies are incorporated into the model to account for inputs such as utilities and catalysts, as well as the output fuels and co-products such as excess electricity, higher alcohols, sulfur and slag. The electricity generated by the plant is used to satisfy its own utility requirements, and any excess electricity is considered a co-product that can be sold to the grid. Slag is sold as construction aggregates [33]. Waste streams generated by the fuel production process, such as spent catalysts and ash, are disposed in landfills, which are

included in the system boundary. Transportation and distribution, and combustion, of the finished MD product make up the last stages of the fuel lifecycle.

2.2 Conversion technologies

This thesis analyzes three thermochemical pathways to convert MSW to MD fuels. Gasification technologies can accept heterogeneous feedstock, including both the biodegradable and non-biodegradable portions of MSW. Although classification to remove inorganics, sizing, and drying of feedstock is necessary for thermochemical pathways, these pre-processing steps can be less energy- and cost-intensive than the pretreatment required for biochemical pathways, wherein the biodegradable and non-biodegradable content of MSW must be separated [12]. Schematics of the pathways are included in Appendix A. The data to calculate the material and energy balances for each pathway are obtained from literature for a facility size of approximately 3000 tonnes per day of raw MSW feed (2000 tonnes per day of dry, processed MSW), based on the size of large landfills in the US that receive more than 30% of the nation's MSW [9].

2.2.1 Conventional gasification and Fischer-Tropsch synthesis

Gasification refers to partial oxidation of the pre-processed feedstock in limited amounts of air or oxygen at elevated temperatures to produce syngas, a mixture of carbon monoxide and hydrogen. The syngas is cooled and conditioned, and then synthesized to fuels and wax using a FT catalyst [34], and the products are refined to yield naphtha, jet and diesel. The naphtha is further reformed to gasoline. The FT process is highly exothermic; the resultant energy as well as

combustion of unconverted syngas is used for feedstock drying and power generation [11, 19]. Conventional gasification and FT are mature technologies [24, 25], with a wealth of literature assessing the use of this pathway for biomass-to-fuel conversion (e.g. [19-27]).

The previous two peer-reviewed works that studied conversion of MSW to MD fuels, Niziolek et al. [11] and Pressley et al. [10], modeled this pathway, and these studies are used to calculate material and energy balances. In order to establish a range of parameter values for uncertainty quantification, this work draws upon additional studies that model this pathway for the production of MD fuels from biomass [19-27]. A number of conversion efficiency scenarios are included in the sensitivity analysis and in Appendix G. Other material inputs and outputs in this pathway include water, catalysts and cleaning chemicals, sulfur cake (sulfur is cleaned from the syngas to prevent poisoning of the FT catalyst) [19] and ash or slag. Bed catalyst materials such as olivine are included in the analysis though their effect is found to be negligible, contributing to less than 1% of the lifecycle GHG emissions and MSP.

2.2.2 Plasma gasification and Fischer-Tropsch synthesis

In the case of plasma gasification, plasma torches are used to create the high temperatures necessary for decomposing and oxidizing the feedstock [35]. Plasma gasification is a less mature technology but because it renders toxic substances non-hazardous and provides cleaner syngas with no tars, it has received considerable interest in waste management [36-38]. Some plasma gasifiers also do not require additional pre-sorting, lowering the feed handling costs [39]. However, as with previous studies of the pathway [35, 37, 40], this analysis includes the same

pretreatment (classification, sizing and drying) procedure as for conventional gasification methods, in order to recycle valuable scrap metals and glass and prevent maintenance challenges.

Only one existing study [40] contains material and energy balance data for this pathway, but several studies have modeled plasma gasification for waste to energy projects [35, 37, 41-44]. This thesis uses the cold gas efficiency data from plasma waste to energy studies by Minutillo et al. and Zhang et al. [37, 42], and combines it with energy balances from FT studies [45, 46] to provide a range of fuel and electricity yields. Other inputs and outputs in this pathway include natural gas, water, catalysts and cleaning chemicals, sulfur cake and slag. Petroleum coke is used as a bed catalyst in this pathway, and is accounted for in the LCA and TEA.

2.2.3 Conventional gasification, catalytic alcohol synthesis and Alcohol-to-Jet

In this pathway, the syngas is converted to ethanol via mixed alcohols synthesis. Higher alcohols such as propanol, butanol and pentanol are produced as by-products. A series of chemical upgrading steps collectively referred to as Alcohol-to-Jet (ATJ), comprising dehydration, oligomerization and hydroprocessing, convert ethanol to jet fuel, diesel and naphtha [47]. Reforming of naphtha to gasoline is included based on a model by Niziolek et al. [11] The fuel yield of the pathway is lower (approximately 25% lower than the FT MD pathway, see Table 2-1) due to low ethanol yields and losses in the additional conversion steps. However, catalytic synthesis of alcohols is less capital-intensive than FT, thereby attracting commercial interest [24]. Enerkem built a full-scale commercial MSW-to-alcohol plant in Edmonton, Canada, but Enerkem uses methanol synthesis instead of mixed alcohols synthesis [48]. The methanol is converted to ethanol via carbonylation and hydrogenolysis [49]. There is limited data

on the Enerkem pathway, and therefore it is only included under the conversion efficiency scenario analysis in Appendix G.

For this pathway, the material and energy balances are determined from a techno-economic study by Jones et al. that models the production of mixed alcohols from MSW [13]. Additional data on material inputs and conversion yields are obtained from LCA and TEA studies that use biomass or waste paper feedstocks for the production of mixed alcohols [50-53]. The ethanol yields are combined with ATJ process balances from Staples et al. to calculate the balances for the overall pathway [47]. The analysis accounts for other inputs and outputs such as water, catalysts and cleaning chemicals, sulfur cake and ash.

2.3 Lifecycle GHG emissions analysis

GHG emissions are calculated as mass of GHG per unit of energy (lower heating value). This thesis considers carbon dioxide (CO_2), methane (CH_4) and nitrous oxide (N_2O) emissions. CH_4 and N_2O emissions are converted into CO_2 equivalents (CO_2e) using the 100-year global warming potentials of the three gases [54]. Climate impacts of non-CO_2 MD fuel combustion emissions are not included in the analysis.

When products use joint processes, emissions are allocated amongst fuels and energy products on the basis of their relative energy contents [55]. This thesis assesses the sensitivity of the LCA results to the allocation approach by comparing results to the displacement method for electricity and higher alcohols co-products, in which excess generated electricity is assumed to displace US average grid electricity, and higher alcohols are assumed to displace virgin higher alcohol production from fossil energy [22, 29, 50]. In order to allocate emissions to non-energy

products, such as elemental sulfur and construction aggregates, the displacement method is used. An alternative method that has been used for allocating emissions among products that are used for dissimilar purposes (such as fuels and construction aggregates) is market-based allocation [8, 47]. However, it is found that for the pathways assessed in this thesis, the use of market-based allocation for these co-products changes mean results by less than 0.01 gCO_2e/MJ compared to the displacement method.

The calculated mass and energy balances are integrated with lifecycle inventories and databases to compute the GHG emissions. Fuel transportation and distribution emissions are obtained from the GREET model (.NET 2015) [29]. Jet and diesel fuel combustion CO_2 emission factors are obtained from the Intergovernmental Panel on Climate Change (IPCC) [56]. The MSW-related emission factors for feedstock transportation, landfill, incineration and recycling, as well as the lifecycle GHG emissions for production of construction aggregates are obtained from the US EPA's WARM model [28]. In order to capture the uncertainty associated with LCA parameters, probability distributions shown in Table 2-1 are employed.

Table 2-1: Parameter distributions for Monte Carlo analysis (Uniform: [Low, High], Triangular/Pert: [Low, Mode, High], Normal: [Mean, Standard deviation], Lognormal: [Log mean, Log standard deviation]). MSW subscript refers to as received raw feed and PMSW subscript refers to pre-processed and dried gasifier feed.

Parameter	Nominal range	Units	Distribution
Pre-processed and dried MSW characteristics			
Energy content (LHV) [57-61]	[19.99,21.79]	MJ/kg_{PMSW}	Uniform
Carbon content [60-64]	[0.48,0.54]	kg/kg_{PMSW}	Uniform
Non-biogenic proportion of carbon [57, 60-64]	[0.37,0.48]	kg/kg_{C}	Uniform
Sulfur content [60-64]	[1.5, 3.4]	g/kg_{PMSW}	Uniform
Ash/inorganic content [60-64]	[0.07,0.14]	kg/kg_{PMSW}	Uniform
Emission factors			
Jet fuel combustion [56]	[69.8,71.5,74.4]	gCO_2e/MJ_{fuel}	Triangular
Diesel fuel combustion [56]	[72.6,74.1,74.8]	gCO_2e/MJ_{fuel}	Triangular
Replaced waste management strategy credit [28, 65]	[-192.31,-167.22,-142.14]	$kgCO_2e/tonne_{MSW}$	Triangular
Recycling credit [6, 28]	[-242.51,-144.55,-77.16]	$kgCO_2e/tonne_{MSW}$	Triangular
US average grid electricity [29, 66]	[144.09,160.1,176.11]	gCO_2e/MJ_{elec}	Triangular
Material and energy process inputs			
Utility for MSW pre-processing [10, 67, 68]	[0.06,0.13,0.15]	MJ/kg_{MSW}	Triangular
Natural gas [40]	[6,0.6]	g/kg_{PMSW}	Normal
Petroleum coke [40]	[50,5]	g/kg_{PMSW}	Normal
Olivine [13, 50, 52]	[1.37,2.07,4.96]	g/kg_{PMSW}	Triangular
Tar reforming catalyst [50-52]	[0.005,0.006,0.045]	g/kg_{PMSW}	Triangular
Material and energy process outputs			
Fuel yield – FT MD [10, 11, 19, 27]	[49.70,53.54,57.16]	$\% MJ_{fuels}/MJ_{MSW}$	Pert
Fuel yield – Plasma FT MD [37, 40, 42, 45, 46]	[32.16,38.45,45.68]	$\% MJ_{fuels}/MJ_{MSW}$	Pert
Fuel yield – ATJ MD [13, 47, 50, 51]	[24.40,31.45,39.96]	$\% MJ_{fuels}/MJ_{MSW}$	Pert
Scrap aluminum [6]	[5.9,14.1,15.1]	g/kg_{MSW}	Triangular
Scrap iron and steel [6]	[3.2,3.6,26.7]	g/kg_{MSW}	Triangular
Scrap glass [6]	[29.6,32.9,45.2]	g/kg_{MSW}	Triangular
Material and energy prices			
Gasoline price in analysis start year (2017) [3]	[0.43,0.57,0.91]	$/L	Pert
Gasoline price growth rate projection [3]	[0.92,2.1,2.32]	%	Pert
Gasoline price yearly deviations [69]	[0,0.077]	$/L	Normal
Natural gas price yearly deviations [69]	[0,74.4]	$/tonne	Normal
Electricity price yearly deviations [69]	[0,0.00314]	$/kWh	Normal
Higher alcohols [53, 70, 71]	[0.34,0.53,0.79]	$/L	Triangular
Petroleum coke [72]	[4.1046,0.1886]	Based on $/tonne	Lognormal
Sulfur [73]	[4.5898,0.3407]	Based on $/tonne	Lognormal
Scrap aluminum [13, 74-77]	[771,1858,2457]	$/tonne	Triangular
Scrap iron and steel [13, 74-77]	[136,342,491]	$/tonne	Triangular
Scrap glass [75, 78]	[7,22,30]	$/tonne	Triangular
Construction aggregates [73]	[7.81,10.20,18.34]	$/tonne	Triangular
Olivine [13, 24, 53]	[234,254,332]	$/tonne	Triangular
Tar reforming catalyst [13, 24, 53]	[12655,15112,20788]	$/tonne	Triangular
Alcohol synthesis catalyst [13, 24, 53]	[12900,14227,15677]	$/tonne	Triangular
Water [13, 79, 80]	[0.10,0.57,0.73]	$/tonne	Triangular
Capital and fixed costs			
Total capital investment – FT MD [11]	[473,598,887]	$M	Pert
Total capital investment – Plasma FT MD [11, 13, 40, 68, 81-83]	[515,643,965]	$M	Pert
Total capital investment – ATJ MD [11, 13, 47]	[302,377,566]	$M	Pert
Fixed operating expenses [53, 81, 84-88]	[4.2,7.74,12.3]	% of total capital	Pert

2.3.1 MSW feedstock characteristics

The US average MSW discards composition in 2013 [6] is used to calculate the feedstock characteristics for the analysis. There are a number of literature references that can be used to calculate lower heating value (LHV) of the feedstock. When using the method presented by the US Energy Information Administration (EIA), the LHV is found to be approximately 13 MJ/kg [57]. The LHV of the pre-processed and dried MSW is approximately 20 MJ/kg. This value and the LHV values calculated using other references are used to establish the probability distribution for LHV [58-61]. Similarly, carbon, ash (inorganic), moisture and sulfur content of the feedstock are calculated [60-64]. An important distinction between MSW and biomass as feedstocks for alternative MD fuel is that a portion of the carbon in MSW is not biogenic by origin, attributable to plastics and rubber [57]. Therefore, the non-biogenic proportion of carbon in the feedstock is calculated to determine the non-biogenic share of process and combustion emissions that have to be counted in the analysis. The MSW composition is not varied for the stochastic analysis because this thesis considers the composition of the total discards in the US as an average representation. Due to lack of uncertainty estimates, arbitrary bounds are not assigned, and instead, sensitivity of results to MSW composition in different cases is assessed.

2.3.2 Replaced waste management strategy

Converting MSW to MD fuels avoids the GHG emissions that would have otherwise resulted from landfilling and incinerating the MSW, but also eliminates existing GHG emission benefits that currently occur if landfill gas is recovered and displaces fossil energy use.

Landfilling waste of biogenic origin releases biogenic CO_2, as well as anthropogenic methane, which would not have otherwise been released. However, depending on the material considered, between 12 and 95% of the carbon in the landfilled waste is sequestered in the soil, which is foregone if MSW is used for MD fuel production. The only GHG emissions associated with landfilled waste of non-biogenic origin are due to transport and machinery usage [89]. Emission factors that account for all of the above effects are obtained from the WARM model for each material type [28]. For landfill gas recovery, the emission factors reported for US average landfill gas recovery rates are used, based on the average landfill type mix. Sensitivity of LCA results to landfill gas recovery rates is assessed.

EPA reports estimates of the composition of MSW that was incinerated or combusted for energy recovery in 2013 [6]. This is combined with WARM model emission factors for combustion with energy recovery to calculate the GHG emissions avoided. The combustion emission factors for each material type take into account non-biogenic combustion CO_2 and N_2O emissions, transportation GHG emissions, avoided electric utility GHG emissions, and avoided emissions due to steel recycling, if applicable [58]. Apart from the materials that are combusted for energy recovery, the remaining discards are assumed to be disposed in landfill. Combining this with the landfill emission factors provides the avoided landfill emissions. For the US 2013 MSW discards composition [6], even after accounting for GHG benefits from landfill gas recovery and carbon sequestration, the net avoided landfill GHG emissions amount to 162 gCO_2e per tonne of raw MSW and the net avoided combustion GHG emissions amount to 5 gCO_2e per tonne of raw MSW [28]. The sum of these is used as the GHG credit from the replaced waste management strategy in this analysis. Lower and upper bounds for the GHG credit are applied for the stochastic analysis based on IPCC guidance [65].

2.3.3 Classification and recycling

The energy requirements for classification and sizing of the MSW feedstock are derived from simulation models of refuse-derived fuel facilities by Pressley et al. and Caputo et al. [10, 67, 68] The inorganics stream that is separated from the MSW feed comprises approximately 55% metals and 30% glass. The composition breakdown by material (ferrous, aluminum etc.) and product type (cans, packaging, durable goods etc.) is used in conjunction with the appropriate GHG emission benefit factors from recycling in the WARM model [6, 28]. For product types that have not been modeled in WARM, similar products are relied on as proxies [90]. In order to capture the associated uncertainties, a range of recycling rates is employed. The rates vary from recycling only aluminum cans, steel cans and glass bottles (approximately 30% of total scrap by weight) at the lower bound to recycling approximately 80% of the total metals and glass by weight. The most likely estimate is assumed to correspond to recycling aluminum cans, aluminum in durable goods (as aluminum ingot), steel cans and glass bottles (approximately 40% of total scrap by weight).

2.3.4 Fuel production process

The material and energy balances calculated for each conversion pathway are used to estimate the process-related GHG emissions, the GHG emissions associated with production of inputs, and the allocation of emissions amongst co-products. Process CO_2 emissions are calculated based on carbon balances. The carbon converted to fuels, alcohols, tars and dissolved hydrocarbons is accounted for and any remaining carbon from the input feedstock and catalysts

is assumed to be converted to CO_2 [50]. GHG emissions associated with production of inputs are determined from the GREET model [29]. The energy product slate used for allocation of emissions by share of energy for each pathway is given in Appendix B. Excess electricity generation is calculated from the literature, and correlated to fuel yield. The result is an inversely proportional relationship since lower fuel yield implies that more unconverted syngas can be combusted for electricity [91].

If the simulation models used to calculate the energy balances for the conversion technologies are missing data on some of the material inputs and outputs, these are estimated with uncertainty ranges from other studies, referenced in Table 2-1. Emissions associated with disposal of rejects, ash and spent catalysts in landfills are accounted for using the WARM model, and since these materials are inorganic they do not contribute to anthropogenic methane emissions [89]. The mass of rejects, ash, slag and sulfur are calculated from the feedstock composition based on sorting efficiency (90%), the calculated inorganic content and sulfur content in pre-processed MSW, as well as elemental sulfur recovery rates from the literature [19].

2.4 Techno-economic analysis

To quantify the economic performance of MD fuels produced from MSW, this analysis calculates minimum selling prices and net present value of plant operation by adopting the discounted cash flow rate of return (DCFROR) model from Pearlson et al. [79] A 20-year plant built using 20% equity financing and a 10-year loan with 10% interest is assumed. The discount rate or cost of capital is assumed to be 15%. The financing assumptions are based on market

research by Blazy et al. [92] An income tax rate of 16.9% is adopted from an empirical analysis by the Government Accountability Office (GAO) [91, 93]. Further financial assumptions are listed in Appendix C. The DCFROR model is solved under these assumptions to find the MSP of MD fuels such that the production facility has an NPV of zero. The MSP provides the MD fuel price that the fuel producer needs to sell at in order to achieve the target rate of return. The DCFROR model is also solved assuming market prices of MD fuels to calculate the NPV of the production. A positive NPV indicates profits above the target rate of return, and a negative NPV indicates profits (or actual losses) below the target rate of return. All prices are expressed in 2014 USD.

The TEA follows the same approach as the LCA in order to consider the results of diverting the MSW to fuel production. The TEA calculates production costs and net present value from the plant perspective (Figure 2-1), and changes to the MSW lifecycle are accounted for if they lead to a change in the costs of inputs or to a change in revenues. The replaced waste management strategy affects the feedstock cost because replacing existing or new landfills may allow the plant to charge similar tipping fees for the MSW feedstock. From the fuel producer perspective this could represent a negative feedstock cost, or a source of revenue. At the same time this could lead to the commodification of MSW and, in the long run, result in a positive feedstock cost. MSW-to-fuel technologies have not entered large-scale commercial production in the US yet, making it difficult to predict future MSW feedstock prices. Existing empirical evidence shows the emergence of long-term, zero-cost MSW feedstock contracts [94], and the present work therefore follows Jones et al. [13], assuming zero feedstock cost for the baseline analysis but quantifying the sensitivity of results to positive and negative feedstock costs.

The economic effect of further classification at the plant is accounted for in terms of revenue generation from the sale of recyclables. Costs of production are calculated at the plant gate, which differ from at-pump prices by the costs of transportation of the fuel to the gas station or airport, and end-user taxes.

2.4.1 Capital cost estimation

Facility capital cost estimates are obtained from the literature referenced for material and energy balances for each pathway [11, 13, 40]. In some cases, the estimates are supplemented with additional capital costs of the processes that are not modeled in the particular studies, such as MSW pre-processing, naphtha reforming to gasoline, and alcohol-to-jet conversion. The capital costs associated with MSW pre-processing are estimated from empirical waste management industry data on equipment costs of RDF facilities and material recovery facilities (MRF) [11, 13, 68, 81-83]. These costs are normalized to the input feed capacity in tonnes/day (approximately $34K for 1 tonne/day feed capacity), contributing 15-25% of the total capital investment for MSW MD fuel production. Due to capacity limits and maintenance requirements, parallel production lines are employed, which limits the potential for economies of scale [95].

The additional capital costs for upgrading naphtha to gasoline are estimated from Niziolek et al. [11] The capital costs of the dehydration, oligomerization and hydroprocessing equipment necessary to convert ethanol to MD fuel are estimated from Staples et al. [47] All capital costs are converted to 2014 USD using the Chemical Engineering Plant Cost Index [96].

2.4.2 Operating costs and revenues estimation

The material and energy balances calculated for the LCA are carried over to the TEA in order to calculate operating costs and sales revenues. The prices of gasoline, jet fuel, diesel, electric power and natural gas are based on EIA historical and projected data [3, 69, 97, 98]. The United States Geological Survey (USGS) mineral commodity summaries provide price estimates for sulfur and construction aggregates [73]. Prices for scrap iron, aluminum and glass are estimated from USGS data, market data from scrap traders, and the literature [13, 74-77]. The price of petroleum coke, water, catalysts and higher alcohols are estimated from the literature cited in Table 2-1. In addition, price estimates for inputs such as cleaning chemicals, water-gas-shift (WGS) catalyst, FT catalyst, pressure swing adsorption packing, and wastewater treatment costs and solid waste disposal costs are obtained from the literature [13, 19, 24, 52]. All prices are adjusted to 2014 US dollars (USD) using consumer and producer price indexes from the Bureau of Labor Statistics (BLS) [99].

Fixed operating costs are estimated as a function of capital expenses. Insurance, local taxes, maintenance and contingency costs are estimated using heuristics from the petroleum refining industry from Gary et al. [88] Employee salary levels, staffing distributions and overhead are estimated from Phillips et al. [53] and adjusted to 2014 USD using the BLS employment cost index [100]. Additional staffing for the MSW classification process at the plant is estimated from empirical data for RDF and MRF facilities [81, 84-87], and a range of estimates is used in order to capture the associated uncertainty. The total fixed operating costs are assumed to vary between approximately 4% and 12% of the capital investment, with 7.7% as the most likely estimate.

2.5 Uncertainty assessment

This thesis implements stochastic analysis using Monte Carlo simulations, wherein parameters are randomly sampled from their probability distributions for 10,000 iterations of the model calculations. This translates the uncertainty in the input parameters to uncertainty in the results. Parameter uncertainty in this study stems primarily from data limitations. Uniform distributions are assigned when available data are considered equally likely. When data is available to estimate minimum and maximum bounds, as well as a most likely value, triangular or pert distributions are assigned. A second type of parameter uncertainty in this analysis is statistical uncertainty associated with availability of a large number of data samples, for example, availability of historical data for commodity prices. In this case, the uncertainty distributions are dictated by the samples, based on best fit using the Anderson-Darling test [101].

2.5.1 Fuel yield uncertainty

The uncertainty associated with the conversion efficiency of the pathway is captured by assigning probability distributions to the overall fuel yield (including MD fuels, gasoline and higher alcohols). Due to lack of empirical data on the fuel yields achievable from commercialized production, previous studies assign pert, triangular or beta general distributions based on theoretical or simulation results reported in literature [91, 102-104]. In this thesis, pert distributions are assumed, similar to Bittner et al. [102], deriving the minimum, maximum and mode values from the literature referenced in Table 2-1. The values calculated from the limited number of MSW-specific studies are typically used as the mode for each pathway, and biomass-

to-MD fuel literature is referred to for other bounds where additional MSW-specific data is not available. Following Motycka, normal probability distributions are assumed for the natural gas and petroleum coke inputs to the Plasma FT MD pathway [40].

2.5.2 Capital cost uncertainty

The capital cost estimates from literature used for this analysis are based on empirical data or chemical engineering models that apply equipment factor estimates and cost all major equipment individually. The error associated with these estimates is typically assumed to be ±20% [88]. Capital costs of similar equipment from biomass-to-MD fuel literature fall within this margin [19-21, 23, 24, 51, 52]. Previous studies that have estimated capital cost uncertainty employed triangular, pert or normal distributions with the point estimate from the capital cost analysis serving as the mode or mean [91, 102, 105, 106]. One approach is to use symmetrical and unbiased probability distributions with the minimum and maximum bounds capturing the accuracy range of the estimation method [106]. However, Brown reports that an asymmetrical distribution with positive skew may be more representative of reality, basing his analysis on the frequency of cost overruns in general energy and construction projects (mean overrun of 5%) [107]. Therefore, a pert distribution is assigned with the point estimate of capital costs as the mode, a lower bound of 80% of this value and the upper bound (150%) is selected to represent a 5% mean overrun.

2.5.3 Fuel and energy price uncertainty

The present work applies Geometric Brownian motion (GBM), as presented in detail in Zhao et al. [91], to project the prices of gasoline, natural gas and electricity from the analysis start year of 2017 until the end of the 20-year valuation period for the plant. A normal distribution is fitted to the year-to-year price variations of the past 20 years from 1996 to 2015. This distribution is randomly sampled from in order to predict price deviations in future years.

The EIA Annual Energy Outlook (AEO) 2015 is referenced to project prices in the analysis start year (2017) and real price growth rates from 2017 to 2037 [3]. The AEO 2015 projects prices for three scenarios: reference, low oil price and high oil price. Uncertainty in 2017 prices and future growth rates is accounted for by assigning pert distributions for both parameters, with the reference scenario values as the modes and the other two scenarios as minimum and maximum bounds. This is implemented for gasoline price and growth projections, and the same parameters for natural gas and electric power are calculated by correlation. Pert distributions are used to assign more of the probability density closer to the mode of the distribution (the reference case). The 2017 prices of gasoline, natural gas and electricity from the AEO 2015 reference case projections are $0.57/L, $5.02/GJ and $0.07/kWh (2014 USD).

Historical data from EIA shows that diesel and jet fuel prices have been highly correlated to the price of gasoline (greater than 99% for wholesale refiner prices) [69]. Therefore, diesel and jet fuel prices are projected for the NPV analysis based on their historical regression relationship with gasoline prices (in $/liter),

$$\text{Diesel price} = 1.1450 \times \text{Gasoline price} - 0.0558, \quad (1)$$

$$\text{Jet fuel price} = 1.1315 \times \text{Gasoline price} - 0.0542. \quad (2)$$

Chapter 3 Results and discussion

3.1 Lifecycle GHG emissions

The results for net lifecycle GHG emissions for the three MSW to MD fuels pathways are summarized in Table 3-1. The median results of 32.86, 62.34 and 52.74 gCO_2e/MJ for FT, Plasma FT, and ATJ MD fuels, respectively indicate that they have the potential to reduce lifecycle GHG emissions compared to the conventional MD baseline of 90 gCO_2e/MJ [108]. However, parameter uncertainty translates into ranges that 95% of the Monte Carlo simulation results lie within: 18.45 – 47.33, 43.55 – 81.47, and 26.44 – 79.32 gCO_2e/MJ, for FT, Plasma FT, and ATJ MD fuels, respectively.

Table 3-1: Lifecycle GHG emissions, MSP and NPV results

	Conversion Pathway	Median	Mean	Std. Dev.
Lifecycle GHG emissions (gCO_2e/MJ)	FT MD	32.86	32.89	7.22
	Plasma FT MD	62.34	62.51	9.48
	ATJ MD	52.74	52.88	13.22
Minimum selling price ($/L)	FT MD	0.99	1.00	0.14
	Plasma FT MD	1.78	1.81	0.29
	ATJ MD	1.20	1.22	0.27
Net present value ($B)	FT MD	-0.339	-0.344	0.312
	Plasma FT MD	-0.753	-0.761	0.252
	ATJ MD	-0.247	-0.247	0.163

The probability density functions of the lifecycle GHG emissions were calculated using MATLAB's kernel smoothing function and are shown in Figure 3-1 [109]. The histograms and estimated skewness and kurtosis of the distributions are given in Appendix D and Appendix E. The conventional gasification and FT pathway has the highest fuel yield of the three pathways; approximately 50-57% of the input MSW energy is converted to fuels (with 54% as the mode of the fuel yield probability distribution). The other two pathways have lower fuel yields, implying that more of the non-biogenic carbon in the MSW feedstock is converted to CO_2 during the process. Higher emissions during fuel production, which are then allocated over lower fuel and energy co-product yields, results in higher net lifecycle GHG emissions for the other two pathways.

Table 3-2 shows the results for each pathway broken out by lifecycle step. The credits from the replaced waste management strategy and recycling are major contributors to the overall GHG emissions. These credits, as well as the emissions associated with feedstock transport, are the same for each of the three pathways on the basis of per tonne of input MSW but vary when they are allocated over the fuel and energy co-product yield. The displacement credit from non-energy co-products, such as sulfur and construction aggregates, contributes less than 0.3% to the net emissions. The emissions associated with disposal of process waste products, and fuel transportation and distribution (T&D) also contribute relatively little to the overall emissions (less than 3% each).

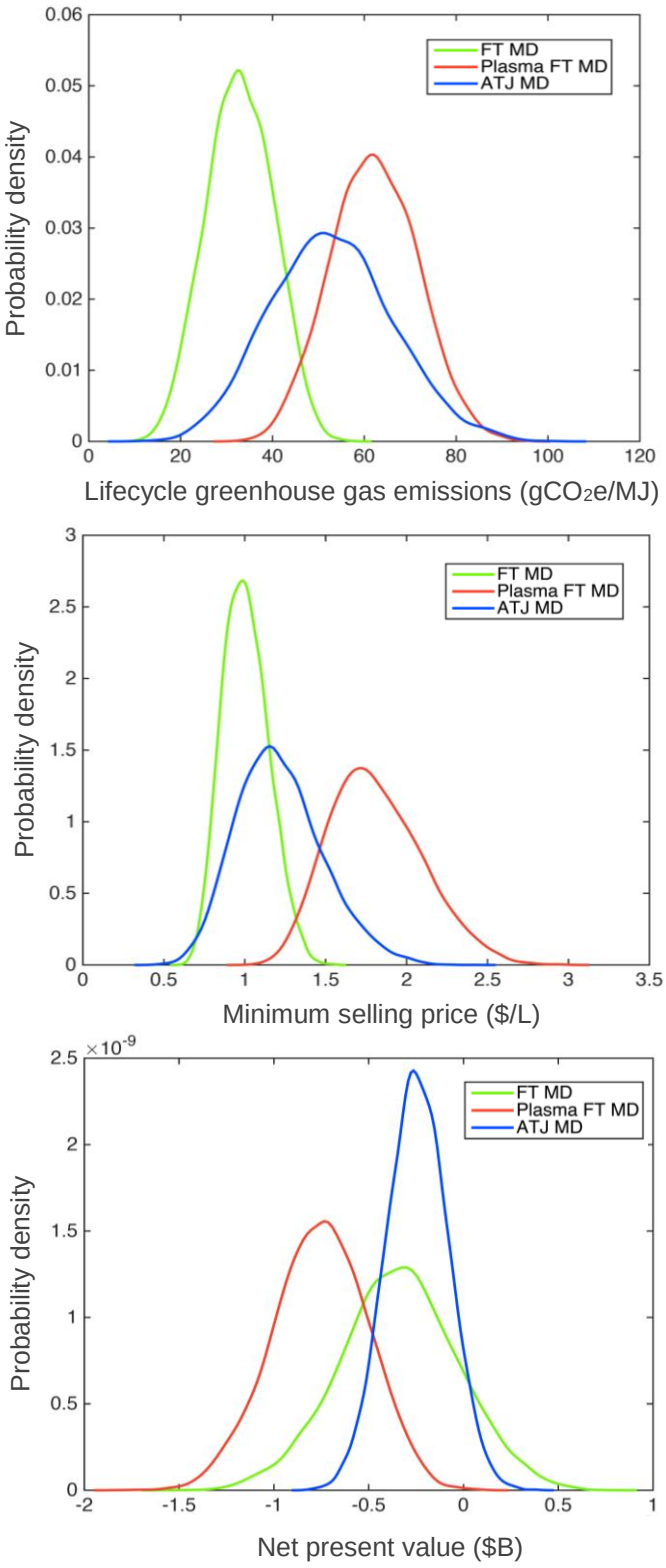

Figure 3-1: Probability (kernel) distributions of the lifecycle GHG emissions, MSP and NPV results

Table 3-2: Lifecycle GHG emissions (gCO_2e/MJ) results breakdown by lifecycle step

	FT MD			**Plasma FT MD**			**ATJ MD**		
	Median	Mean	Std. Dev.	Median	Mean	Std. Dev.	Median	Mean	Std. Dev.
Replaced waste management strategy	-22.09	-22.11	1.53	-27.17	-27.27	2.06	-40.13	-40.31	4.36
Additional recycling	-20.11	-20.41	4.53	-24.88	-25.28	5.63	-36.61	-37.21	8.87
Non-energy co-products	-0.10	-0.10	0.02	-0.12	-0.12	0.02	-0.02	-0.03	0.01
Feedstock transport	3.76	3.76	0.13	4.61	4.64	0.20	6.84	6.85	0.61
Fuel production	39.05	39.21	4.20	74.24	74.85	7.22	89.95	90.76	12.54
Disposal of rejects, ash and waste	0.38	0.38	0.03	0.46	0.46	0.04	1.15	1.16	0.12
Fuel T&D and combustion	32.14	32.15	2.17	35.25	35.23	2.03	31.67	31.66	2.15

The fuel production and combustion steps are major sources of GHG emissions in all three pathways. The Plasma FT MD pathway has the highest fuel production emissions per tonne of input MSW. The mode of the fuel yield probability distribution for this pathway is approximately 38%. At this fuel yield, the pathway generates more excess electricity than the other pathways (almost 9% of the input MSW energy) but at the upper bound of fuel yield of 46%, the plant has to import electricity to meet plasma power requirements. This results in increased net GHG emissions due to the high carbon intensity of the US average grid mix (160.1 gCO_2e/MJ) [29]. Fossil fuel inputs such as petroleum coke and natural gas further increase the GHG emissions associated with fuel production in this pathway.

For the ATJ MD pathway, the fuel yields vary between 24 – 40% of the input MSW energy with 31% as the mode, the lowest of the three pathways. Therefore, on a per MJ of MD fuel basis it has higher fuel production emissions, which are offset by higher credits per MJ, resulting in a 15% lower median GHG emissions than the Plasma FT MD pathway. Fuel combustion emissions attributable to the non-biogenic portion of the MSW feedstock are similar for the three pathways and vary only because of the different proportions of diesel and jet fuel produced by each pathway. Different combustion CO_2 emission factors are used for the two fuels from IPCC [56].

In addition to the standard deviation measures listed in Table 3-2, this thesis also quantifies the contributions of the parameters that are sampled for the stochastic analysis to the overall variance of the results. Uncertainty associated with the non-biogenic proportion of carbon in the feedstock contributes approximately 47%, 41% and 41% of the total variance of lifecycle GHG emissions for FT, Plasma FT, and ATJ MD fuels, respectively. This translates to larger standard deviations for the fuel production and combustion steps where the non-biogenic share

of emissions is counted. Other major contributions to variance are 39%, 34% and 38% from the recycling credit; 8%, 8% and 9% from the feedstock carbon content; 1%, 8% and 8% from fuel yield; and 4%, 3% and 4% from the replaced waste management strategy credit for FT, Plasma FT, and ATJ MD fuels, respectively. Detailed results are presented in Appendix F.

Sensitivity analysis is conducted to quantify variability within the pathways. Figure 3-2 shows the five drivers that are assessed by varying each one in isolation. The parameter that produces the largest change in results for all three pathways is the MSW composition, characterized by the non-biogenic proportion of carbon in the feedstock and the LHV of the feedstock. The 0% non-biogenic case assumes absence of all plastics and rubber. This reduces the energy content of the feedstock to approximately 8 MJ/kg, and is accompanied by a reduction of almost 40% in the quantity of fuel produced per tonne of raw MSW, relative to the baseline. Overall, the absence of non-biogenic carbon emissions during fuel production and combustion reduces the median lifecycle GHG emissions by 180-320% overall, depending on the pathway. The 65% non-biogenic case assumes the absence of food wastes, yard wastes and wood, and this reduces the replaced waste management credit since the landfill emissions due to these biogenic wastes are not avoided. Additionally, the non-biogenic CO_2 emissions from both fuel production and combustion are higher, resulting in a net increase of 60-100% in the median lifecycle GHG emissions. These results reflect the sensitivity of lifecycle GHG emissions of the MSW MD fuels to variability in the composition of MSW that may occur in different geographic regions.

In the baseline case, US national average landfill gas recovery rates have been assumed in order to calculate the replaced waste management credit in the baseline stochastic analysis. Figure 3-2 shows two other potential cases: one with no landfill gas recovery (replaced waste management credit of 603 kgCO_2e per tonne of MSW) and the other with all replaced landfills

assumed to have landfill gas recovery for energy with aggressive gas collection. In the latter case, replacing the waste management strategy results in GHG emissions of 23 $kgCO_2e$/tonne [28].

For the conventional gasification and FT pathway, material and energy balances are estimated for a larger facility scale from Larson et al. [11] and a different fuel yield case at the same 3000 tpd scale from Vliet et al. [26] At the larger 7000 tonne per day (tpd) feed capacity scale, a lower fuel yield of 34% (23% excess electricity) leads to higher lifecycle GHG emissions by approximately 11 gCO_2e/MJ compared to the baseline median. On the other hand, generating additional excess electricity while maintaining high fuel yield (52% fuels and 8% excess electricity) at the 3000 tpd scale, results in lower net GHG emissions (31.5 gCO_2e/MJ).

In the case of the plasma gasification and FT pathway, the 1000 tpd facility with a fuel yield similar to the baseline generates additional excess electricity, and therefore has lower lifecycle GHG emissions (by 8%) [44, 45]. The second case assesses the effect of increased fuel yield at the 3000 tpd scale that requires additional electricity to be imported from the grid [37, 45], resulting in 56% higher lifecycle GHG emissions. Due to data limitations, this work assesses only the effect of different conversion efficiencies for the ATJ MD fuel pathway. The higher fuel yield is based on future projections by Mu et al. [50] and the lower fuel yield is based on the conservative estimate by Jones et al. [13], which also forms the lower bound in the uncertainty assessment. These cases and other conversion efficiency scenarios are detailed in Appendix G.

Using the displacement method instead of energy allocation generates a carbon credit for the excess electricity exported to the grid, and the produced higher alcohols, making the Plasma FT and ATJ MD pathways more sensitive than the FT MD pathway to the emissions allocation method. The baseline analysis uses the default feedstock transport distance of 20 miles from the

EPA WARM model. Varying the parameter between 10 and 70 miles based on literature estimates correspondingly reduces (4-8%) and increases the associated emissions (21-37%) [110].

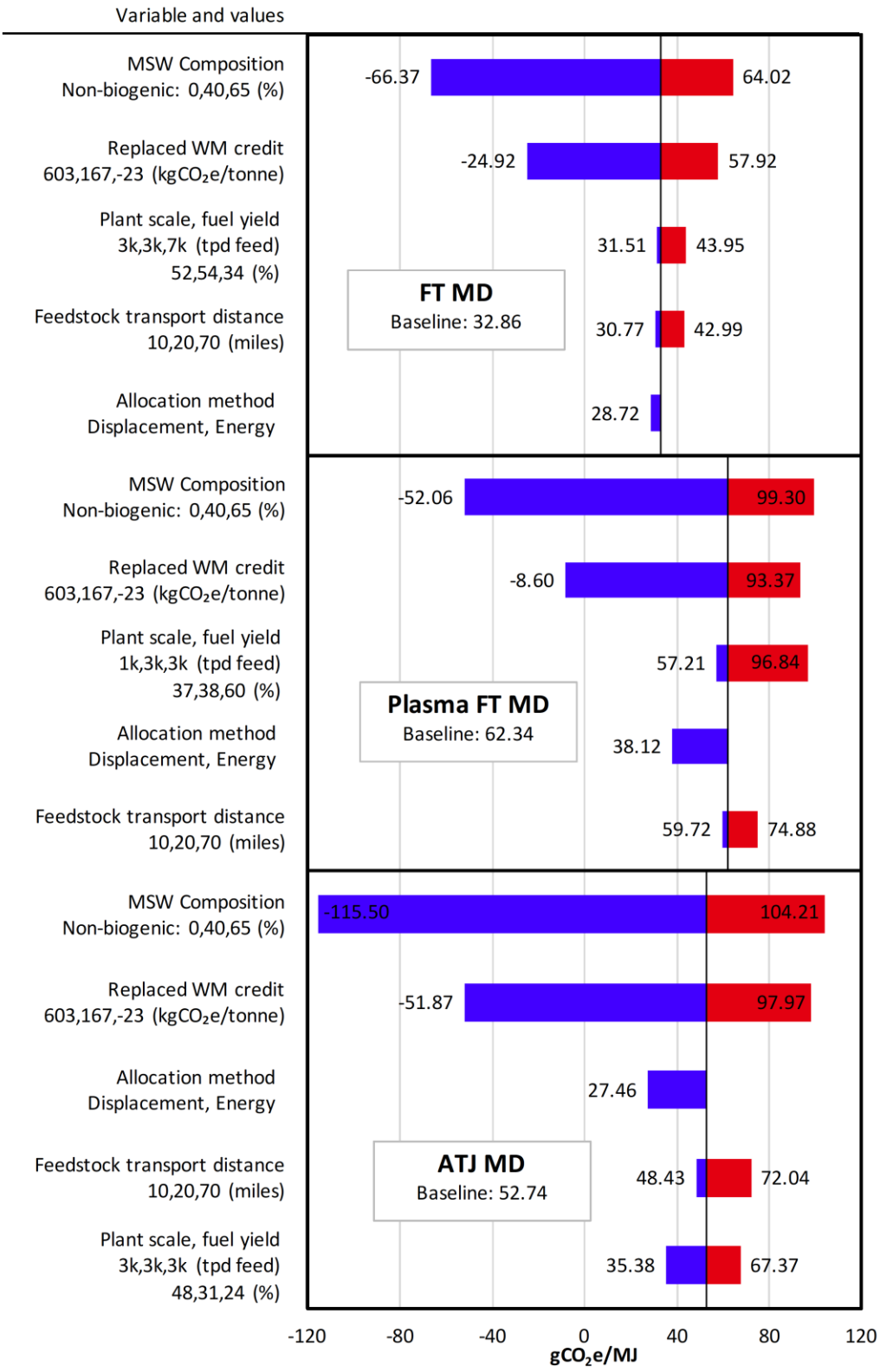

Figure 3-2: Lifecycle GHG emissions sensitivity analysis showing the resultant median values. The variables and assumptions are listed on the left axis (low, baseline, high).

3.2 Minimum selling price and net present value

The MSP and NPV results for the three MSW to MD fuels pathways are summarized in Table 3-1. The median MSP results are 0.99, 1.78 and 1.20 $ per liter for FT, Plasma FT and ATJ MD fuels, respectively. Parameter uncertainty results in ranges of values that 95% of the Monte Carlo simulation results lie within: 0.72 – 1.28, 1.24 – 2.39 and 0.68 – 1.75 $ per liter for FT, Plasma FT, and ATJ MD fuels, respectively. These results, even at the lower bound, are above the approximate average US price of conventional middle distillate fuel in January 2016 of 0.27 $ per liter (refiner price) [69]. However, there is volatility associated with fuel prices in the short and long term, and this volatility is accounted for in the NPV calculations. The probability of achieving positive NPV for the project is calculated from the NPV results to be 14%, 0.1% and 7% for FT, Plasma FT, and ATJ MD fuels, respectively.

The probability density functions (kernel distribution) of the MSP and NPV results are shown in Figure 3-1, and the histograms and estimations of skewness and kurtosis are provided in Appendix D and Appendix E. Table 3-3 and Table 3-4 show the results for each pathway, disaggregated by type of cost and type of revenue. Capital costs and fixed operating expenses, which are a function of the capital costs, are the major cost contributors for all three pathways, making up 70-75% of total expenses. The net capital costs are highest for the Plasma FT MD pathway and the lowest for the ATJ MD pathway but when normalized to the MD fuel yield, the FT MD pathway has the lowest median capital cost per liter of $0.89/L.

The variable operating expenses attributable to water, catalysts, cleaning chemicals and disposal of wastes are only 2-3% of MSP for all three pathways. Comparison of the results indicates that revenues from the sale of gasoline, and of scrap metals and glass, vary among the

three pathways due to technology-specific differences in conversion process product slates and plant feed capacities. The Plasma FT and ATJ MD pathways have higher co-product revenues from higher export of excess electricity and sale of higher alcohols, respectively (see Table 3-4). Non-energy co-products such as slag and construction aggregates contribute less than 3% to reducing the overall cost.

Similar to the LCA results, contributions to variance are quantified for the MSP and NPV results. The major contributions to variance of MSP are 73%, 70% and 54% from capital costs; 11%, 10% and 10% from fixed operating costs; 3%, 12% and 24% from fuel yield; and 3%, 2% and 3% from the price of scrap aluminum for FT, Plasma FT, and ATJ MD fuels, respectively. The primary contributions to variance of NPV are 51%, 35% and 35% from year-to-year fuel price variations; 21%, 14% and 15% from the analysis start year (2017) fuel prices; 20%, 40% and 30% from capital costs; 3%, 6% and 5% from fixed operating costs; and 1%, 1% and 6% from fuel yield for FT, Plasma FT, and ATJ MD fuels, respectively. Detailed results are presented in Appendix F.

The majority of variance in the NPV results arises from uncertainty associated with fuel prices. Since the fuel yields are higher for the FT MD pathway, the total variance and standard deviation are also greater than that of the other two pathways. On the other hand, the MSP of the FT MD pathway has the lowest standard deviation (0.14 $/L) of the three pathways because calculation of the MSP divides the net costs over the fuel yield, thereby resulting in an inverse relationship. Following from the fuel yields and the capital costs (shown in Table 2-1 and explained in Section 3.1), the FT MD fuel has the lowest median MSP and the Plasma FT MD fuel has the highest median MSP of the three pathways.

Table 3-3: MSP ($/L) results breakdown by cost and revenue contributors

	FT MD			Plasma FT MD			ATJ MD		
	Median	Mean	Std. Dev.	Median	Mean	Std. Dev.	Median	Mean	Std. Dev.
Capital costs	0.89	0.91	0.113	1.75	1.77	0.248	1.41	1.43	0.221
Fixed operating expenses	0.25	0.25	0.048	0.47	0.48	0.099	0.39	0.39	0.083
Variable operating expenses	0.02	0.02	0.001	0.06	0.06	0.008	0.02	0.02	0.008
Income tax	0.10	0.10	0.013	0.20	0.21	0.028	0.16	0.17	0.025
Revenue from gasoline	-0.12	-0.12	0.019	-0.31	-0.32	0.046	-0.22	-0.22	-0.032
Revenue from scrap recyclables	-0.13	-0.13	0.030	-0.20	-0.21	0.051	-0.30	-0.30	-0.079
Revenue from other co-products	-0.03	-0.03	0.004	-0.20	-0.18	0.065	-0.27	-0.27	-0.046

Table 3-4: NPV ($M) results breakdown by cost and revenue contributors

	FT MD			Plasma FT MD			ATJ MD		
	Median	Mean	Std. Dev.	Median	Mean	Std. Dev.	Median	Mean	Std. Dev.
Capital costs	-1206.9	-1221.2	148.3	-1312.2	-1328.6	161.1	-769.9	-779.3	94.5
Fixed operating expenses	-330.6	-331.7	63.0	-358.8	-361.5	69.3	-212.6	-213.7	40.5
Variable operating expenses	-30.2	-30.3	1.2	-43.0	-43.9	6.8	-11.8	-13.7	5.6
Income tax	-74.6	-79.1	49.4	-25.6	-30.1	24.9	-42.1	-44.3	24.3
Revenue from MD fuels	976.3	987.7	287.0	542.9	548.0	163.7	393.9	399.3	121.3
Revenue from gasoline	123.2	124.6	33.7	168.5	169.9	47.5	86.4	87.5	24.9
Revenue from scrap recyclables	169.4	170.5	40.5	154.0	154.8	36.9	166.1	166.6	39.6
Revenue from other co-products	34.5	35.0	5.0	143.2	130.4	42.3	148.7	150.8	27.3

The ATJ MD pathway has the least negative median NPV because the relative reduction of net capital costs outweighs other costs compared to the other two pathways. However, to achieve a positive NPV, the ATJ MD pathway requires a higher selling price for the fuel than the FT MD pathway, because the lower fuel yield implies that each unit of fuel needs to be sold at a higher price.

Figure 3-3 presents the results of the sensitivity analysis for the MSP and NPV in terms of discount rate, income tax rate, feedstock cost, plant scale and associated technology parameters, and carbon pricing as an example of a policy driver (detailed results are provided in Appendix H). The discount rate, which is dictated by the rate of required return for equity and loan interest rate for debt, has the greatest impact on the results. From an investor's perspective, Blazy et al. suggest that the discount rate could be up to approximately 22% for novel alternative fuel technologies with significant associated risks [92]. This reduces the probability of positive NPV to 0-0.4% and increases the MSP by 40-60% depending on the conversion pathway. To assess sensitivity in the opposite direction, the social opportunity cost of capital is used based on long-term treasury bond rates from the US Office of Management and Budget as the discount rate (3.2% nominal) [111]. This decreases the MSP by 50-70%, and increases the probability of positive NPV above 80% for the FT and ATJ MD pathways.

The plant scale and conversion yield cases assessed for NPV and MSP are the same as for the LCA sensitivity analysis, except for the FT MD pathway, wherein the 3000 tpd case (other than the baseline) considered for the economic sensitivity analysis is based on data from Zhu et al. [24] At larger feed input capacities, economies of scale are achieved for the conversion technologies. At the same feed capacity and level of capital investment, improvements in fuel yield increase the probability of positive NPV to greater than 50%. In the case of the FT MD

pathway, at the same feed capacity, lower fuel yield (39%) and 8% higher capital costs than the baseline results in a decrease of the probability of positive NPV to 0.4%.

In order to quantify the impact of feedstock cost, the 2013 US average landfill tipping fees is used [6], first as a source of revenue that lowers the median MSP by 20-46% and raises the probability of positive NPV to 2.5-55% and second, as a positive cost associated with the feedstock as it gains value due to end-use as fuels, yielding the opposite effect. The latter increases the median MSP by 25-50% and lowers the probability of positive NPV to 0-2%. Income tax expenses have a similar effect, raising the median MSP by 24-32% when the tax rate is raised to match the 2015 US combined corporate income tax rate of 39%, as reported by OECD [112]. In the discount rate and feedstock cost cases, the ATJ MD pathway demonstrates the lowest median MSPs ($0.34/L, $0.64/L) and highest probability of positive NPV (87%, 55%) compared to the other two pathways.

Figure 3-3 also presents the results of implementing a carbon price of $48.56 (2014 dollars) based on the revised social cost of carbon guidance provided by the US Interagency Working Group on Social Cost of Carbon [113]. This ties together the results of the LCA and TEA analyses. The carbon price improves the median MSP of the FT MD pathway by 11% compared to 3-4% for the other two pathways because of its greater lifecycle GHG savings potential of 63% compared to 30-40% (median estimates).

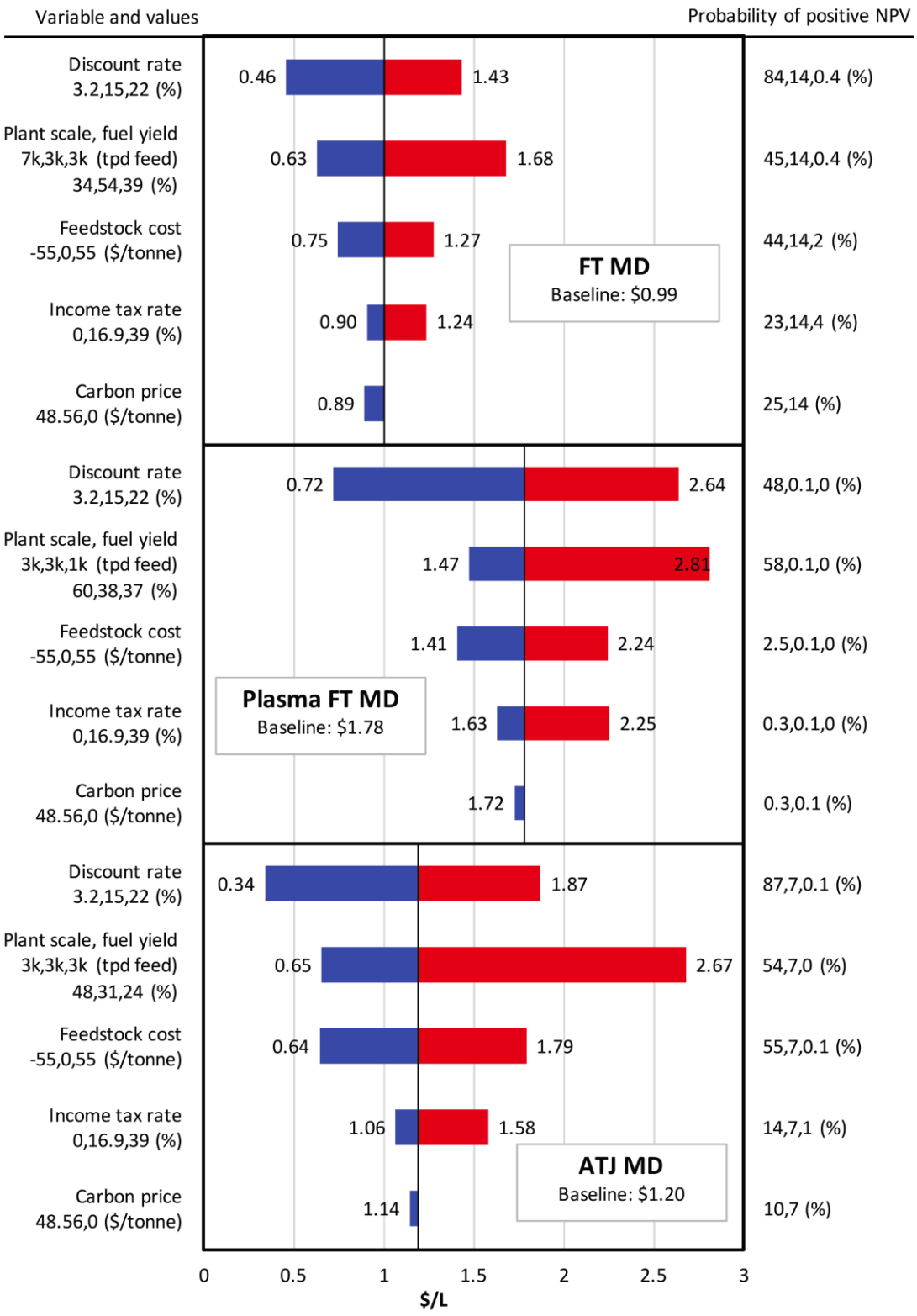

Figure 3-3: MSP sensitivity analysis showing the resultant median values. The variables and assumptions are listed on the left axis (low, baseline, high). On the right axis, the probability of positive NPV associated with each case (low, baseline, high) is listed.

Chapter 4 Conclusions

This thesis quantifies the lifecycle GHG emissions and costs of production of diesel and jet fuels derived from MSW via three thermochemical pathways. The results show that MSW MD fuels have potential to reduce lifecycle GHG emissions when compared to conventional diesel and jet fuels. Although there is substantial parameter uncertainty, the probability of lifecycle GHG emissions from MSW MD exceeding lifecycle GHG emissions from conventional MD fuels baseline is less than 0.5%. The lifecycle GHG emissions can be minimized by technology selection and improvement in conversion pathway efficiencies. The mature conventional gasification and FT technologies demonstrate higher conversion efficiencies in the literature, leading to the lowest median lifecycle GHG emissions of the three pathways (32.86 gCO_2e/MJ). Improving fuel yields while maintaining sufficient electricity generation to meet the plant's utility needs could reduce the lifecycle GHG emissions of all three pathways.

Drawing a larger system boundary allows for analysis of the change in GHG emissions that occurs due to conversion of MSW to fuels, relative to the existing waste management strategy. Therefore, the total lifecycle GHG emissions of the MSW MD fuels are dependent on the waste management being replaced, credits from additional recycling, and combustion emissions attributable to the non-biogenic content of the feedstock. The results presented in this thesis represent the current US average characteristics of MSW feedstock; the MSW composition and credit from replaced waste management strategies may vary significantly at different spatial and temporal scopes [9, 114].

The results of the TEA show that MSW MD fuels have higher costs of production than conventional MD fuels. The probability of positive NPV is less than 15% for all three pathways. Based on capital costs and conversion yields, the conventional gasification and FT pathway has the greatest probability of positive NPV (14%) and lowest median MSP ($0.99/L). MSP can be reduced, and NPV increased, by improving conversion efficiencies and the sale of recyclables for all three pathways. The ATJ MD pathway has the lowest net capital costs for the scale considered, and therefore, the least negative median NPV of -247 million USD.

This analysis accounts for the volatility associated with conventional petroleum-derived MD fuel prices in the NPV analysis, and it is noted that MSW MD fuels will be more economically attractive if conventional MD fuel prices rise over time. Moreover, being able to charge fees similar to landfill tipping fees for the MSW feedstock can improve economic viability. However, in the absence of higher crude oil prices and feedstock-related revenues, policy mechanisms will be necessary to improve the economic feasibility of MSW MD fuels. For example, policy incentives that enable de-risking of the investment through loan guarantees and offtake agreements can lower the discount rate. Other potential policy mechanisms may include tax waivers, capital subsidies, low carbon fuel standard and carbon pricing. Carbon pricing is of particular interest in this work because it combines the lifecycle GHG emissions results and economic results by assigning an economic value to the GHG benefits of MSW MD fuels. Based on the results of the sensitivity analysis, if the societal perspective is considered rather than an investor's perspective, assuming the social opportunity cost of capital, corporate income tax waivers and implementation of carbon pricing, the probability of positive NPV increases to 93%, 67% and 92.5% for the FT, Plasma FT, and ATJ MD pathways, respectively.

This work only addresses lifecycle GHG emissions, whereas additional analyses could include criteria such as air quality and non-GHG climate impacts [115]. Furthermore, this work compares the GHG benefits of MSW MD fuels only to conventional petroleum-derived fuels, and not to MSW-to-electricity or MSW-to-ethanol pathways. The GHG benefits of different waste management strategies depend on a number of factors, such as MSW composition, carbon intensity of the grid electricity, conversion efficiencies and feedstock pretreatment requirements [116, 117].

The results of this analysis indicate that diesel and jet fuels produced from MSW offer the potential to reduce the GHG emissions intensity of transportation, but policy mechanisms may be necessary to ensure economic viability. There is significant uncertainty associated with the results because the technologies are still in the early stages of development and are yet to be commercialized. Therefore, the uncertainty and variability of parameters should be taken into account for decision-making and technology selection. For example, the FT MD pathway may be more economically attractive at a 15% cost of capital rate but the ATJ MD pathway may become more attractive at lower discount rates or when feedstock revenues are available. Overcoming the technical and economic challenges, the impacts of which have been quantified in this thesis, will be key to commercializing diesel and jet fuel production from MSW.

Appendix A Conversion pathway schematics

The following schematics show the major conversion processes, inputs and outputs, based on models from literature [10, 11, 13, 19, 37, 40, 42, 50, 51]. Heat and power inputs and generation (by combustion of unconverted syngas and/or steam cycle) are not shown, since the processes vary between the literature models for each pathway. However, net power requirement or generation is incorporated into the analysis. High temperature gasification produces slag whereas low temperature gasification produces ash. Water, wastewater and wastes such as spent catalyst beds are also not shown in the schematics, but are accounted for in the analysis.

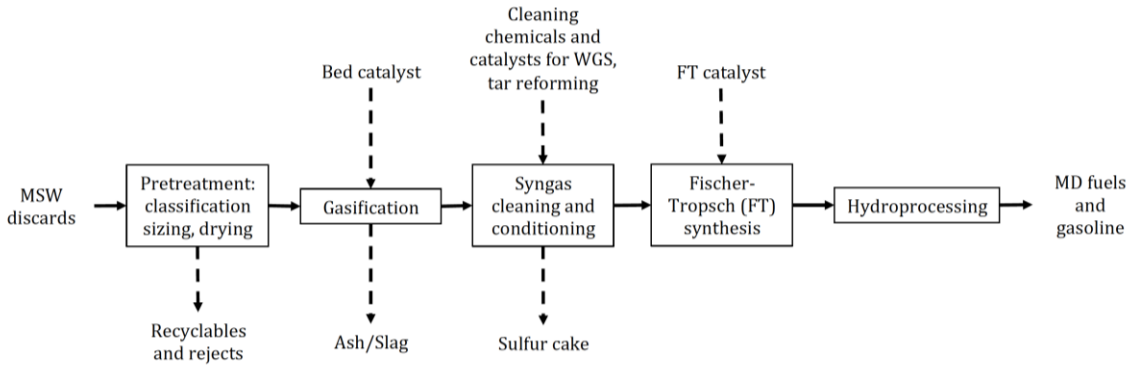

(a)

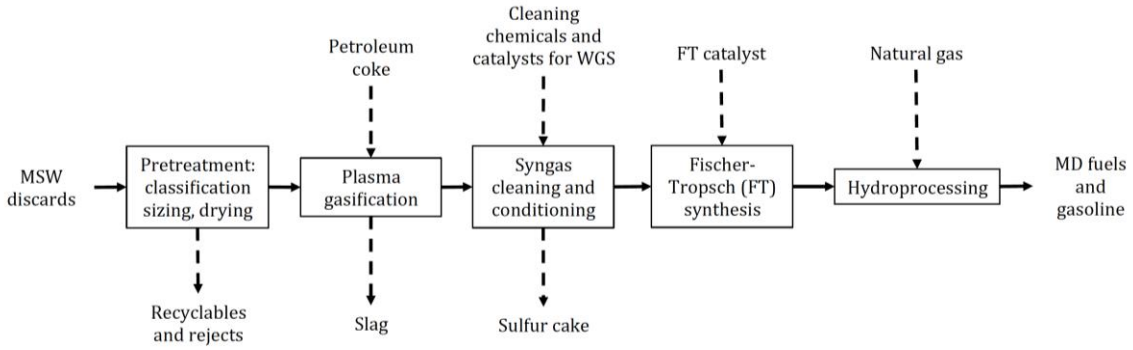

(b)

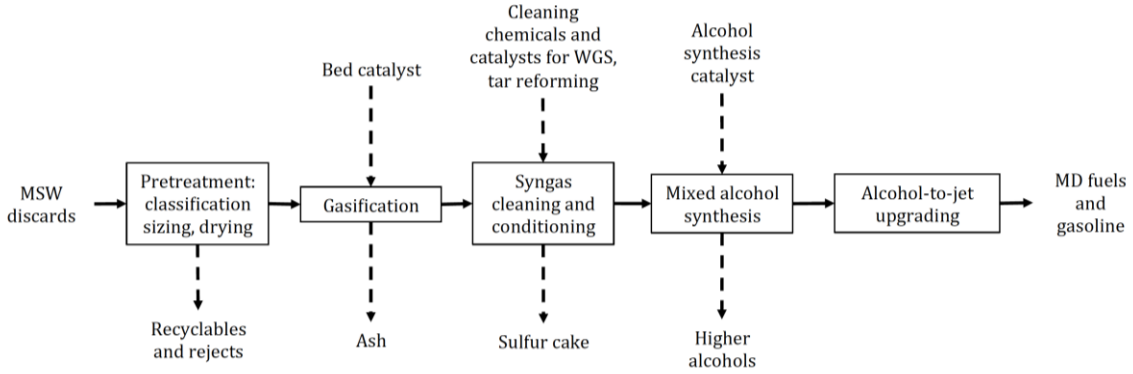

(c)

Figure A-1: Schematics of the MSW to MD fuel pathways considered in this study, (a) FT MD, (b) Plasma FT MD, (c) ATJ MD

Appendix B Energy product slates

For each pathway, the share of energy of each product in the energy product slate is used for allocation of GHG emissions. Table B-1 below details the energy share of the product slate corresponding to the mode of the fuel yield probability distribution. For the uncertainty analysis, the overall fuel yield is varied but the energy split of jet fuel, diesel, gasoline and higher alcohols as proportions of the overall fuel yield remains constant. The excess electricity yield values vary inversely with overall fuel yield. Note that the excess electricity yield values listed here are not inclusive of the utility requirement for additional sorting (see Table 2-1 for the latter parameter's distribution).

Table B-1: Proportion of product in the energy product slate by share of energy for the FT, Plasma FT and ATJ MD pathways

Energy product	FT MD [10, 11]	Plasma FT MD [40]	ATJ MD [13, 47]
Jet fuel	12.0%	26.2%	48.1%
Diesel	73.0%	35.7%	13.1%
Gasoline	10.7%	19.3%	13.6%
Excess electricity	4.0%	18.8%	2.2%
Higher alcohols	0%	0%	23.0%

Appendix C Economic assumptions for techno-economic analysis

Table C-1: Financial and economic assumptions adopted for calculation of MSP and NPV

Parameter	Assumption
Equity fraction [92]	20%
Loan term [92]	10 years
Loan interest rate [92]	10%
Discount rate (nominal) [92]	15%
Inflation rate [79]	2%
Working capital [79]	5% of total capital investment
Depreciation period [79]	10 years
Depreciation method [79]	Variable declining balance
Construction period [79]	3 years
Proportion of capital expenses in year 1 of construction [79]	8%
Proportion of capital expenses in year 2 of construction [79]	60%
Proportion of capital expenses in year 3 of construction [79]	32%
Income tax rate [91, 93]	16.9%
Production ramp-up: Startup period [91]	6 months
Startup production rate [91]	50%
Startup variable costs [91]	75%
Startup fixed costs [91]	100%
Plant operating level [11, 118]	90% (330 days/year)

Appendix D Histograms of the Monte Carlo simulation results

This section presents the lifecycle GHG emissions, minimum selling price and net present value results in the form of histograms. The height of each bar in the histograms represents the relative number of iterations for which the results fall within the bin. The bar heights add up to 1 [119].

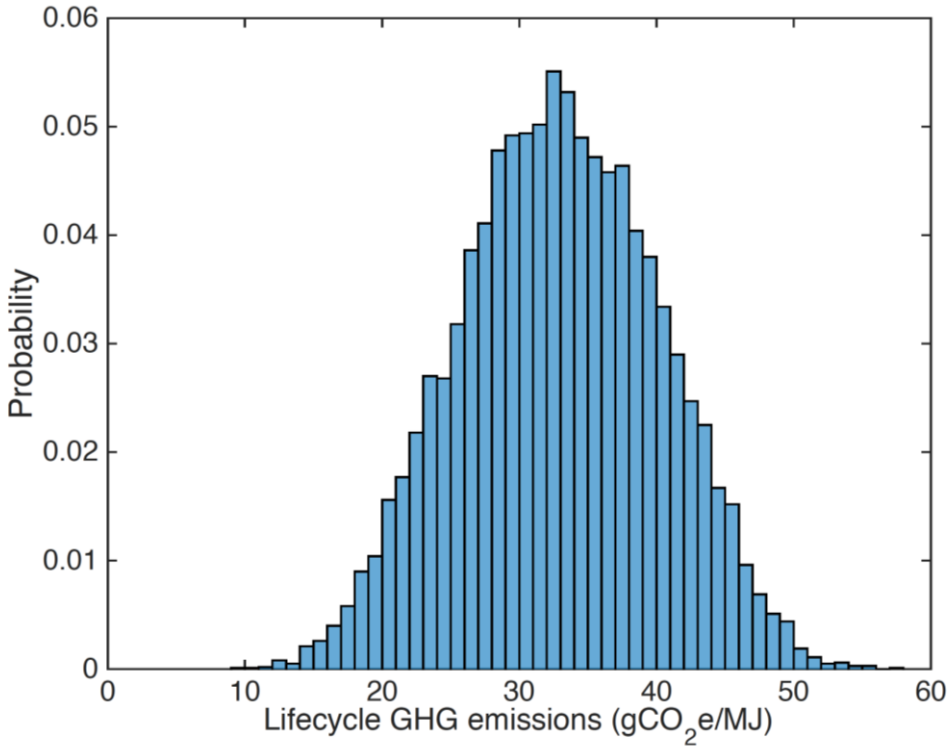

Figure D-1: Histogram of the lifecycle GHG emissions results of FT MD fuel

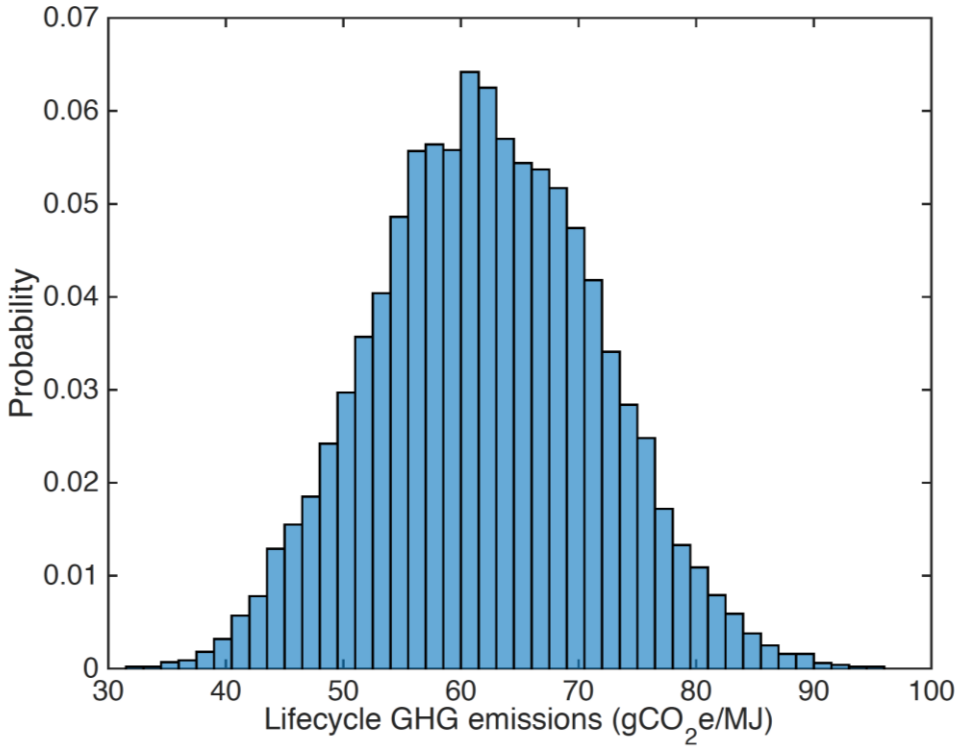

Figure D-2: Histogram of the lifecycle GHG emissions results of Plasma FT MD fuel

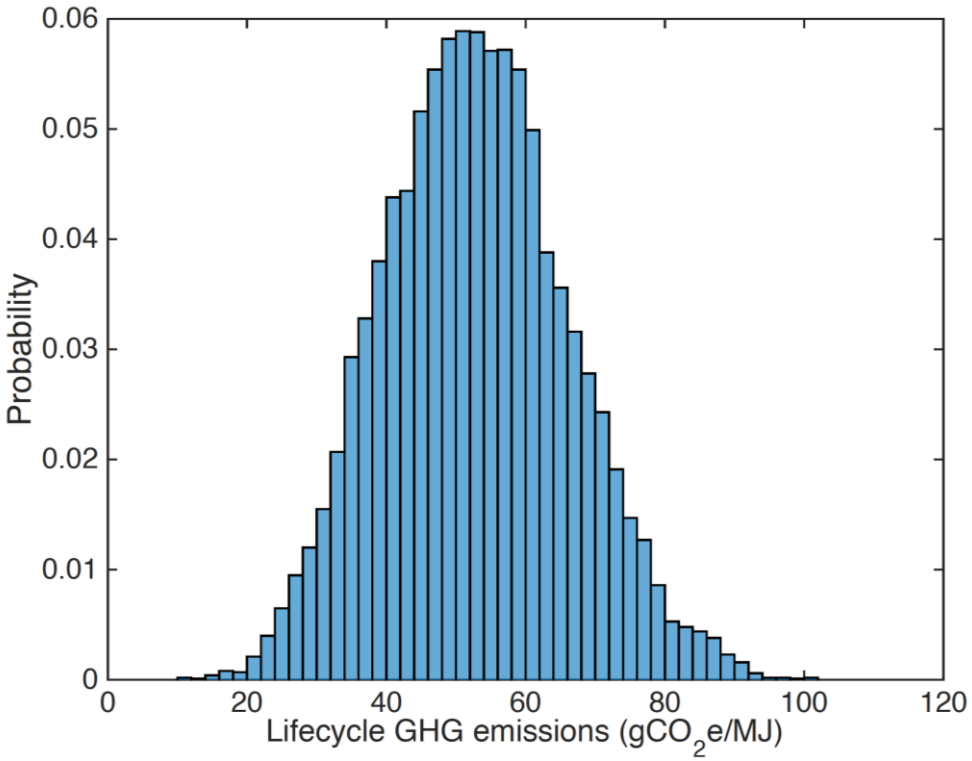

Figure D-3: Histogram of the lifecycle GHG emissions results of ATJ MD fuel

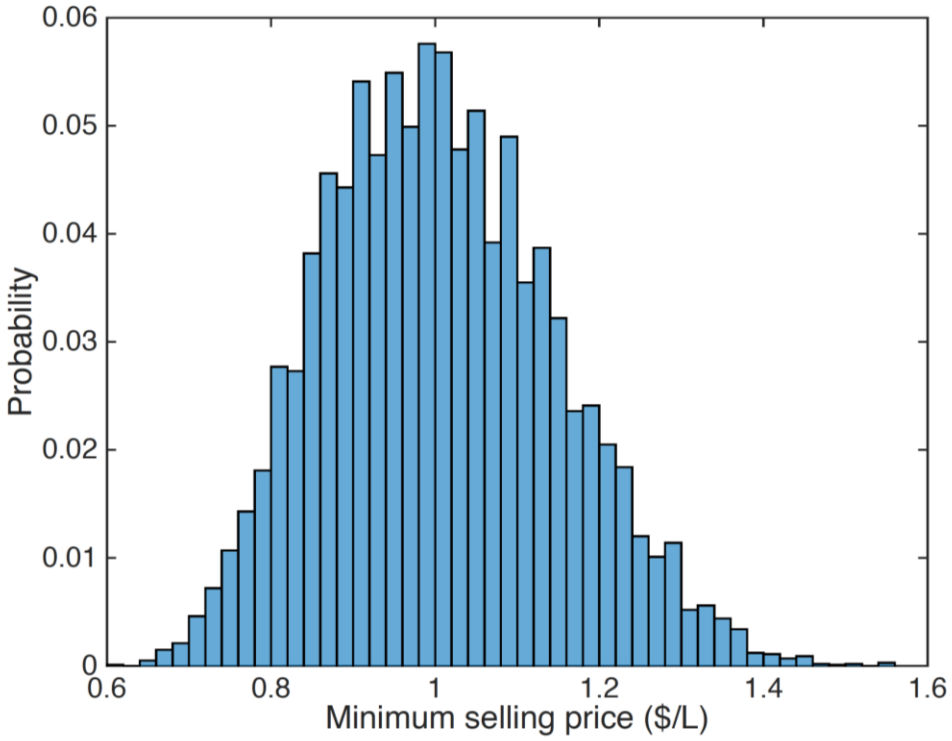

Figure D-4: Histogram of the MSP results of FT MD fuel

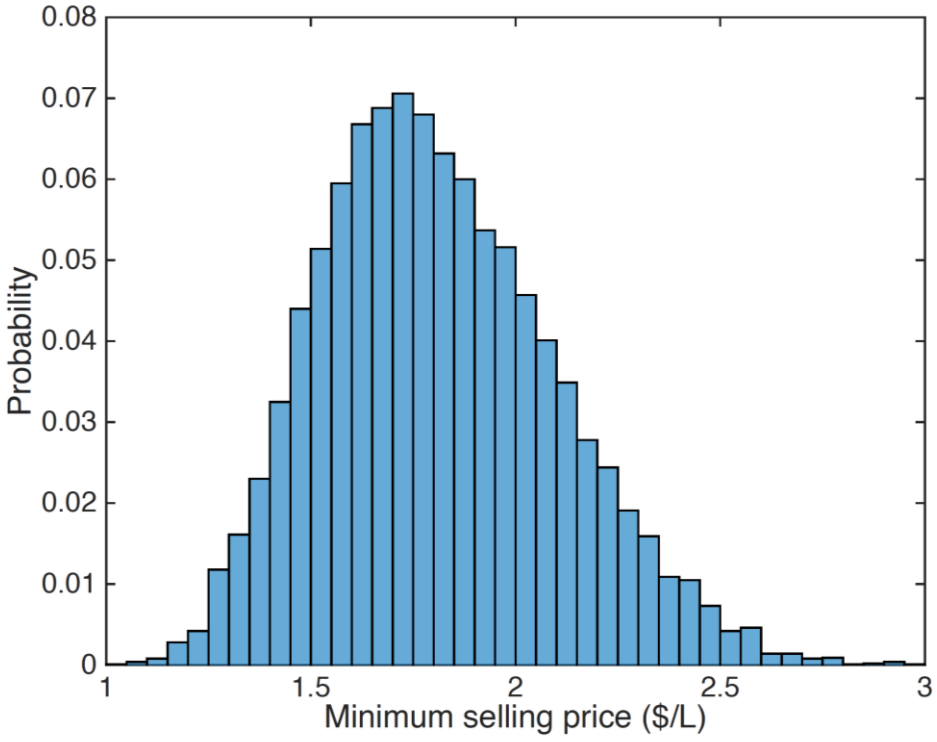

Figure D-5: Histogram of the MSP results of Plasma FT MD fuel

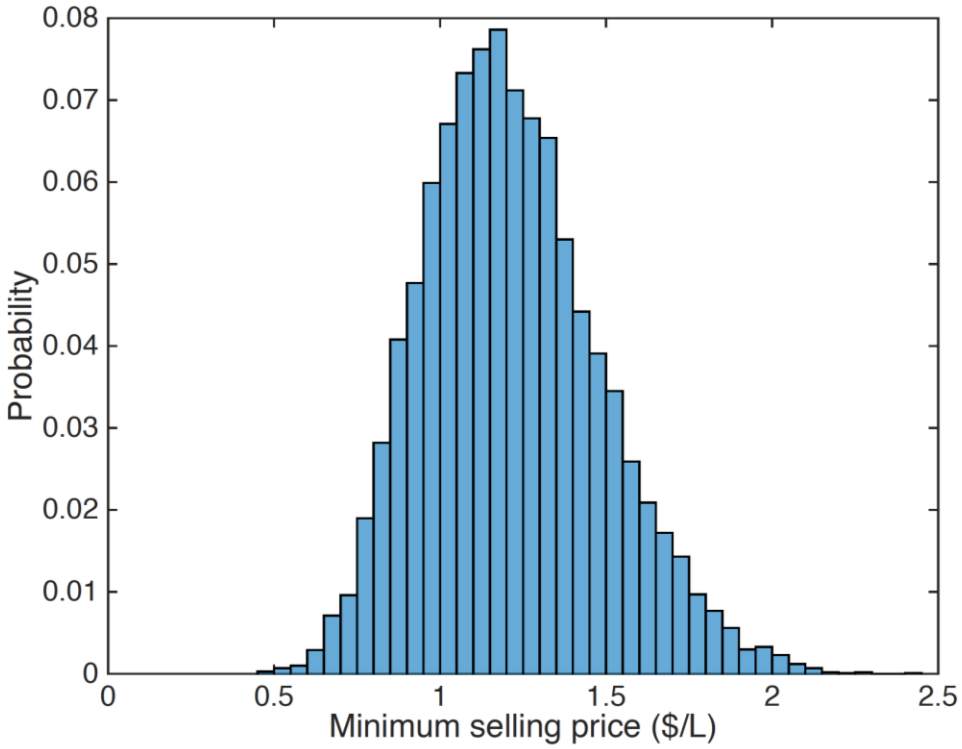

Figure D-6: Histogram of the MSP results of ATJ MD fuel

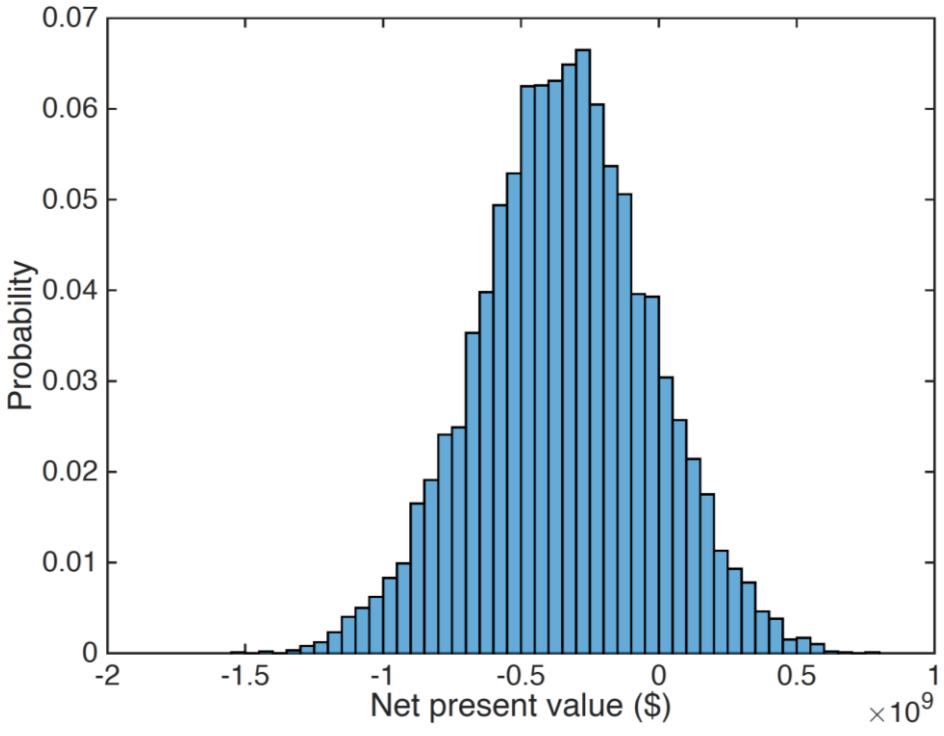

Figure D-7: Histogram of the NPV results of FT MD fuel

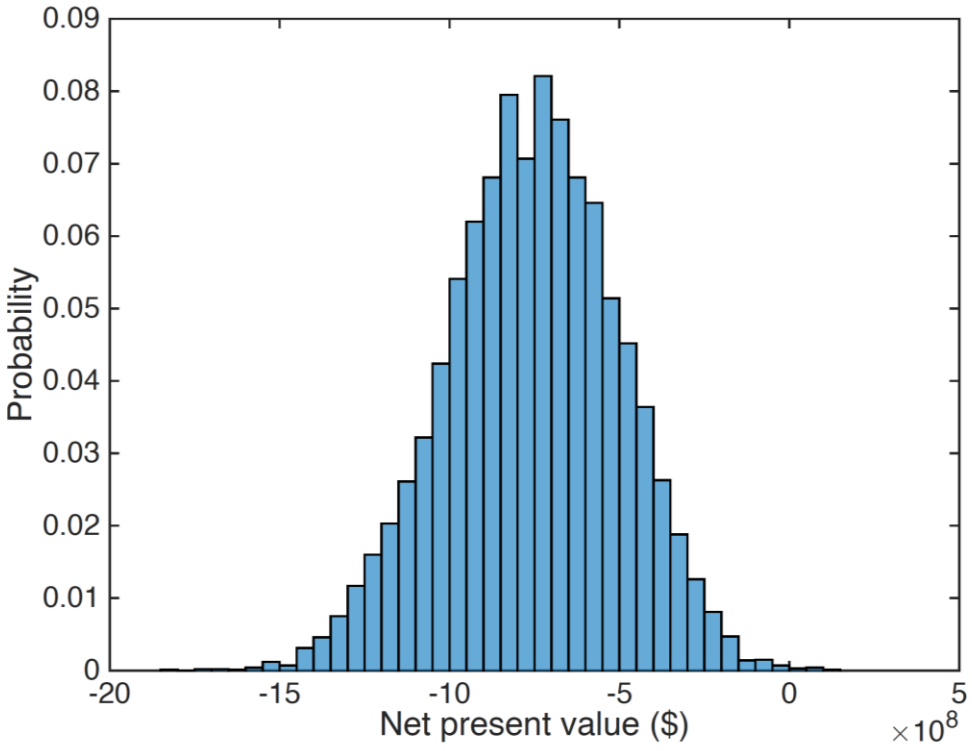

Figure D-8: Histogram of the NPV results of Plasma FT MD fuel

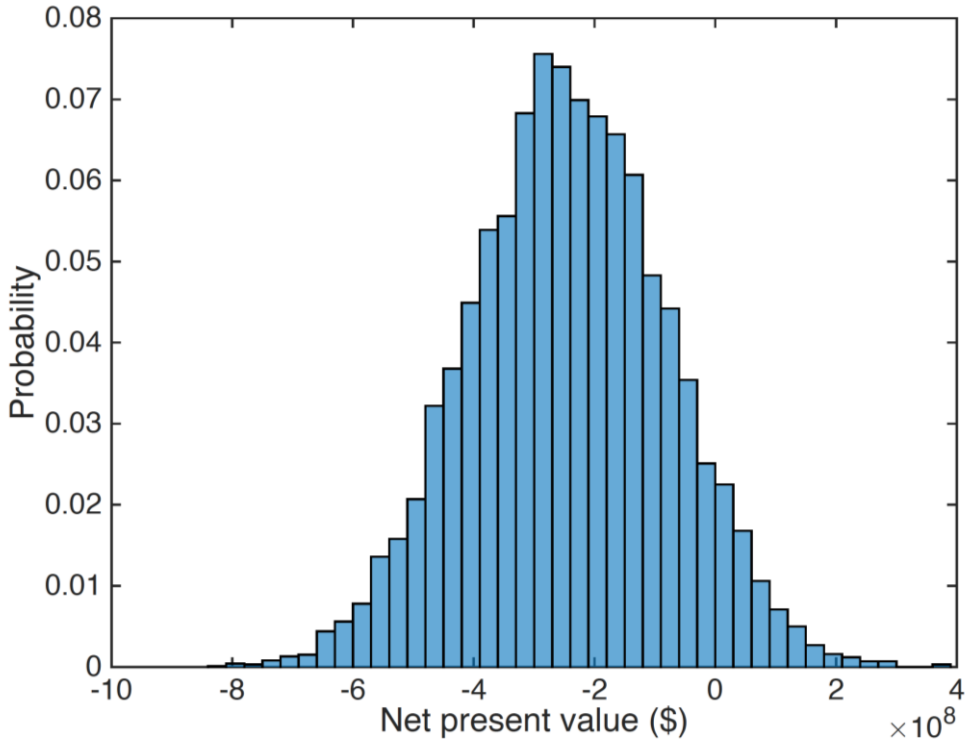

Figure D-9: Histogram of the NPV results of ATJ MD fuel

Appendix E Skewness and kurtosis of the Monte Carlo simulation results

Skewness measures the asymmetry of the results about the mean and kurtosis measures how outlier-prone a distribution is. The skewness of a normal distribution is 0 and the kurtosis of a normal distribution is 3 [120, 121]. Skewness between -0.5 and 0.5 indicates that the distribution is approximately symmetric [122]. As shown in Table E-1, the skewness measures of the lifecycle GHG emissions and net present value results are well within this margin. This is reflected in Figure E-1 and Figure E-3, where the estimated probability distributions (kernel density) are compared to fitted normal probability distributions [109]. However, the minimum selling price results display positive skewness closer to 0.5 and the shift from the normal distribution can be observed in Figure E-2. The minimum selling price distributions are skewed positive/right primarily due to the positive skew of the capital investment probability distribution. The net present value distributions do not display similar skewness because the variance contributions from fuel price uncertainty are greater than the variance contributions from capital cost uncertainty (quantified in Appendix F).

The kurtosis of the resultant distributions is similar to that of normal distributions (approximately 3), as shown in Table E-1. The lifecycle GHG emissions distributions are slightly platykurtic (negative kurtosis with reference to the normal distribution, i.e. kurtosis value lower than 3) [123]. Distributions with negative kurtosis have lower, flatter peaks and lighter tails, indicating that the distribution may be less outlier-prone or that less of the variance is due to

extreme values as compared to the normal distribution [123, 124]. The minimum selling price distribution for the FT MD pathway is also slightly platykurtic.

Table E-1: Skewness and kurtosis measures of the Monte Carlo simulation results for lifecycle GHG emissions, MSP and NPV. Skewness and kurtosis are unitless measures.

	Conversion Pathway	Skewness	Kurtosis
Lifecycle GHG emissions	FT MD	-0.0072	2.6318
	Plasma FT MD	0.0709	2.7871
	ATJ MD	0.1701	2.8591
Minimum selling price	FT MD	0.2967	2.7898
	Plasma FT MD	0.4145	2.9386
	ATJ MD	0.4371	3.1163
Net present value	FT MD	-0.0264	2.9802
	Plasma FT MD	-0.1239	2.9413
	ATJ MD	0.0094	2.9682

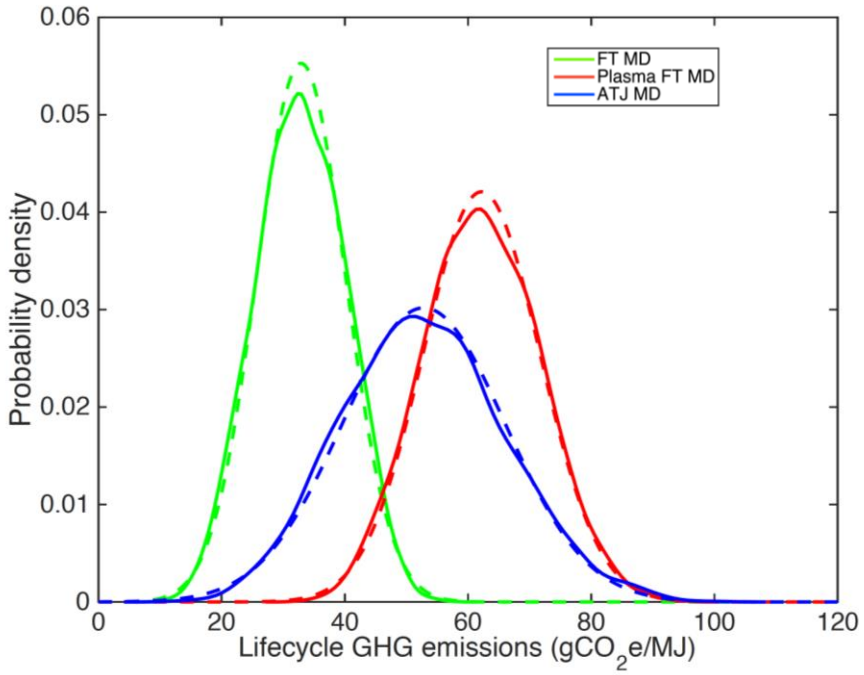

Figure E-1: Probability distributions of the lifecycle GHG emissions results of FT, Plasma FT and ATJ MD fuels. The solid lines represent the kernel-estimated distributions and the dashed lines represent normal distributions fitted to the data.

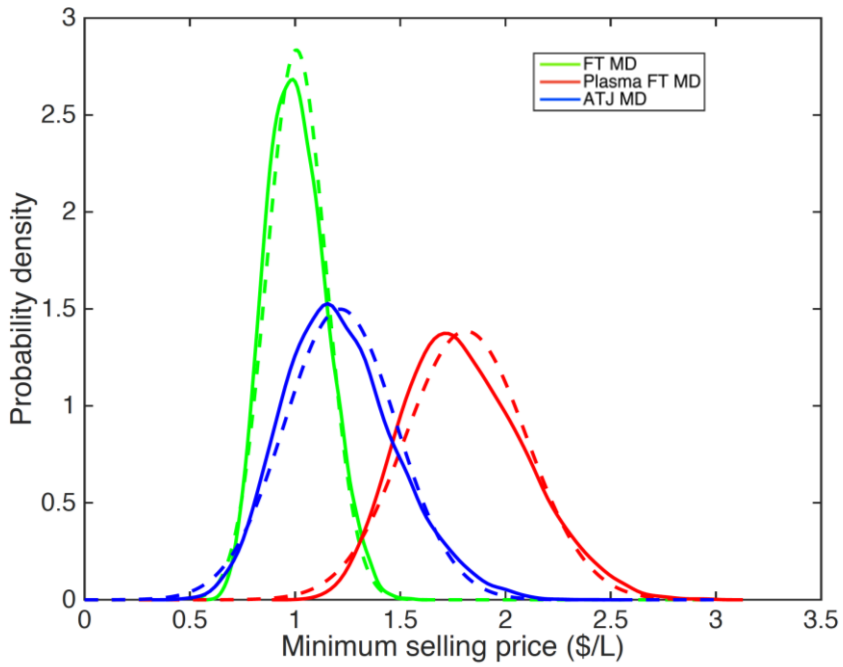

Figure E-2: Probability distributions of the MSP results of FT, Plasma FT and ATJ MD fuels. The solid lines represent the kernel-estimated distributions and the dashed lines represent normal distributions fitted to the data.

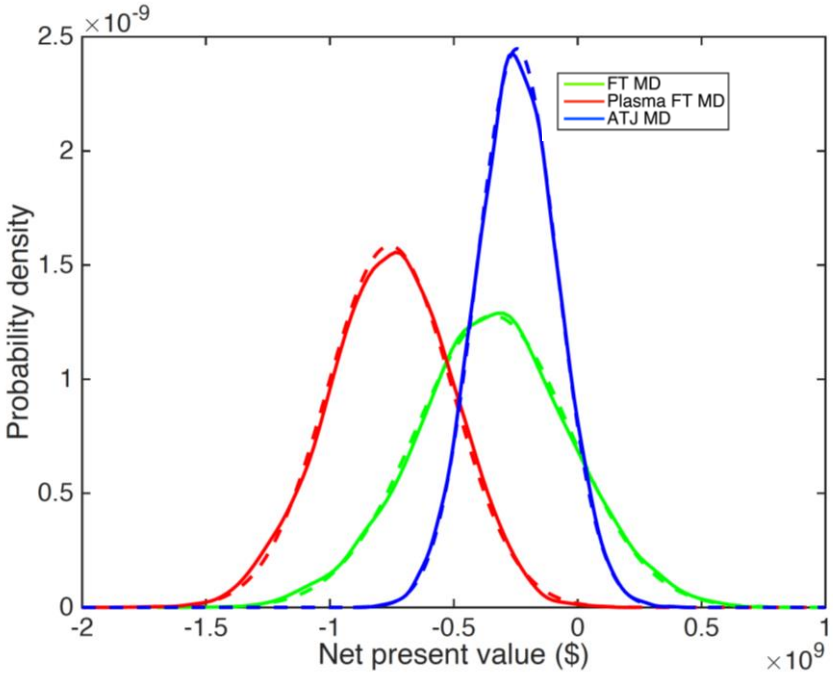

Figure E-3: Probability distributions of the NPV results of FT, Plasma FT and ATJ MD fuels. The solid lines represent the kernel-estimated distributions and the dashed lines represent normal distributions fitted to the data.

Appendix F Contributions to variance

This section details the contributions of parameter uncertainty to overall variance of lifecycle GHG emissions, minimum selling price and net present value results for the three conversion pathways.

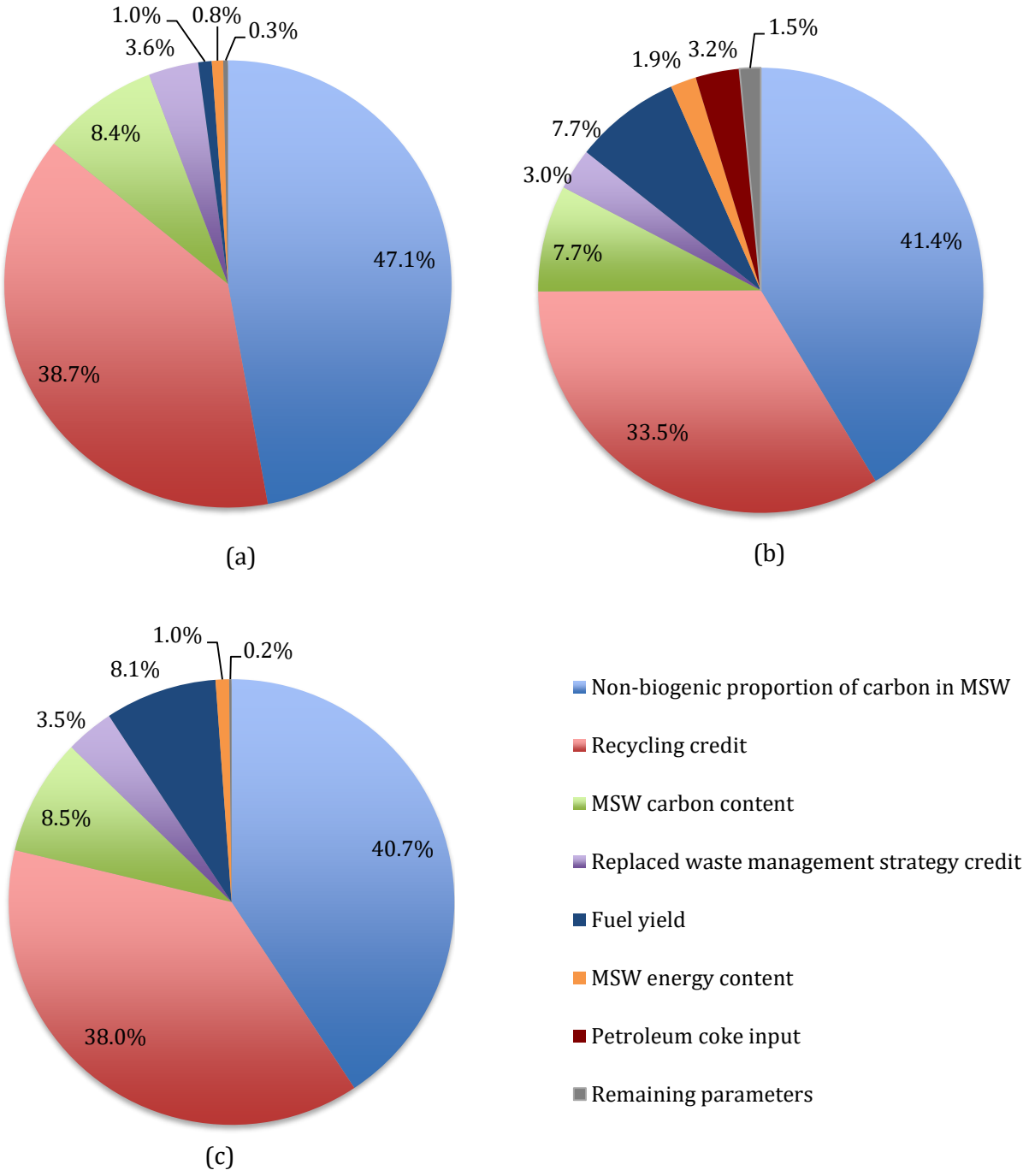

Figure F-1: Contributions to variance of lifecycle GHG emissions results for (a) FT MD, (b) Plasma FT MD, and (c) ATJ MD fuels

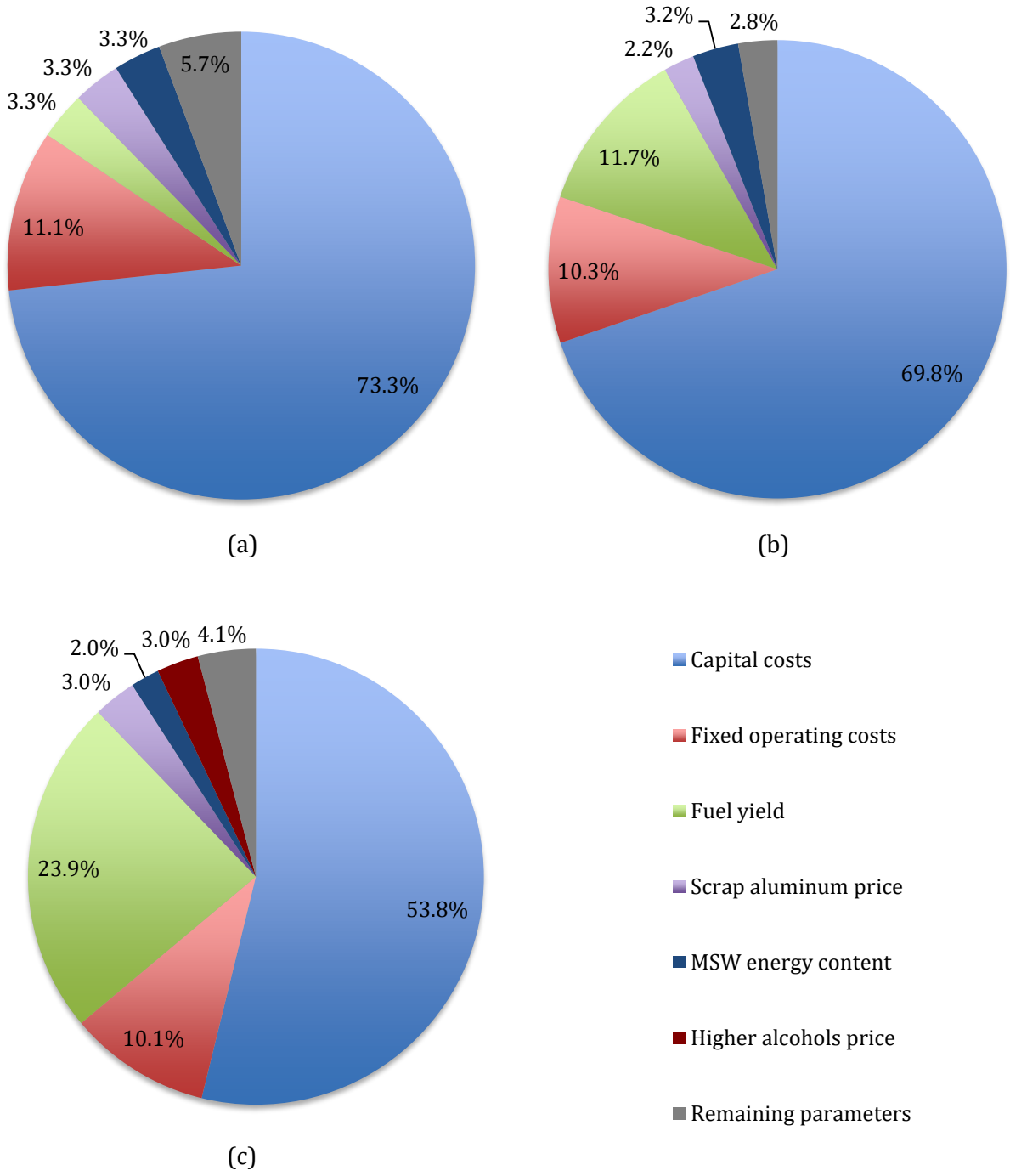

Figure F-2: Contributions to variance of MSP results for (a) FT MD, (b) Plasma FT MD, and (c) ATJ MD fuels

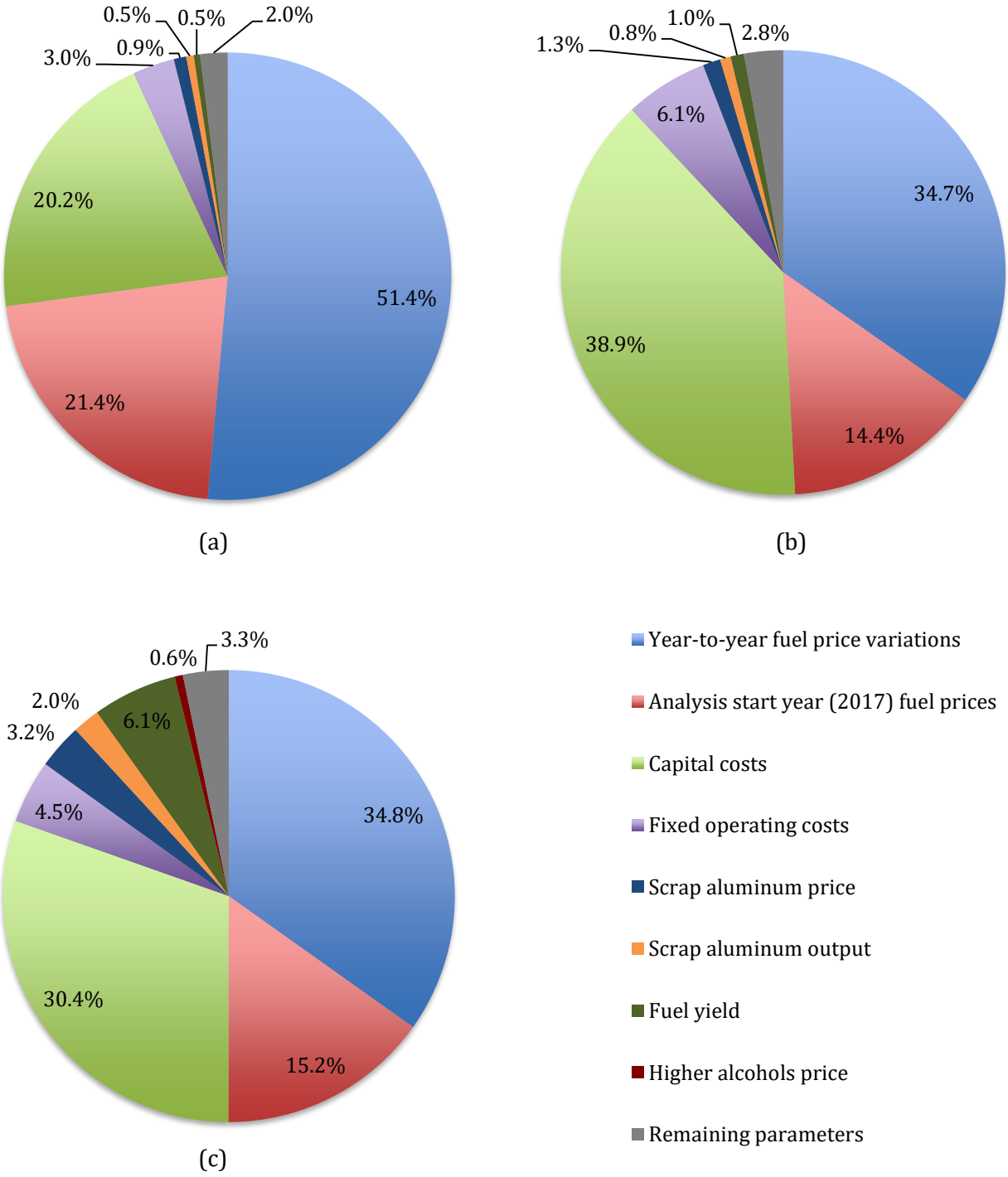

Figure F-3: Contributions to variance of NPV results for (a) FT MD, (b) Plasma FT MD, and (c) ATJ MD fuels

Appendix G Sensitivity of results to conversion efficiency parameters

In the following tables, the conversion efficiency parameters are calculated directly from the cited sources or estimated in combination with other references. The electricity yield values listed here are not inclusive of the utility requirement for additional sorting (see Table 2-1 for the parameter's distribution). The net electricity yield is positive if excess electricity is generated and negative if additional electricity has to be imported from the grid. The results are calculated with the deterministic point estimates for the conversion yields given in the tables and pert distributions for the total capital investment with the estimate in the tables as the mode, the minimum being 80% of the mode and the maximum being 150% of the mode. All other parameters are randomly sampled based on their probability distributions from Table 2-1. Note that 'MSW' subscript refers to as received raw feed and 'PMSW' subscript refers to pre-processed and dried gasifier feed.

Table G-1: Conversion efficiency parameters and results for the FT MD pathway. The baseline is based on the case from Pressley et al. [10] (combined with data from Niziolek et al. [11]). The cases that are demonstrated in the sensitivity analysis are the 7000 tpd case from Larson et al. [21], the case from Vliet et al. [26] and the case from Zhu et al. [24]

		Pressley et al. [10]	Vliet et al. [26]	Swanson et al. [19]	Kreutz et al. [20]	Larson et al. [21]	Zhu et al. [24]	Hamelinck et al. [23]
Conversion yields and other parameters	Scale (tpd_{MSW})	3200 [11]	2500	3100	4300	7000	3100	3500
	Jet fuel (MJ/MJ_{PMSW})	6.8%	0.0%	0.0%	0.0%	0.0%	0.0%	0.0%
	Diesel (MJ/MJ_{PMSW})	16.0%	44.2%	34.9%	28.1%	21.1%	30.4%	28.13%
	Gasoline (MJ/MJ_{PMSW})	30.8%	7.8%	14.8%	18.1%	13.1%	8.8%	4.38%
	Net electricity (MJ/MJ_{PMSW})	2.2%	7.9%	3.5%	5.7%	23.1%	6.4%	12.3%
	Total capital investment ($M)	597 [11]	522	684	844	1015	643	532
Lifecycle GHG emissions (gCO_2e/MJ)	Median	32.48	31.51	37.61	33.27	43.95	45.63	47.54
	Mean	32.50	31.58	37.62	33.23	44.02	45.67	47.43
	Standard deviation	7.09	6.65	7.52	7.51	7.46	8.84	9.02
Minimum selling price ($/L)	Median	1.00	1.29	1.48	1.35	0.63	1.68	1.13
	Mean	1.01	1.31	1.49	1.36	0.65	1.69	1.14
	Standard deviation	0.32	0.18	0.23	0.26	0.27	0.25	0.19
Net present value ($B)	Median	-0.336	-0.456	-0.656	-0.675	-0.056	-0.701	-0.312
	Mean	-0.338	-0.458	-0.662	-0.683	-0.055	-0.707	-0.315
	Standard deviation	0.310	0.230	0.300	0.384	0.454	0.263	0.227
Probability of positive NPV		14%	2%	1%	4%	45%	0.4%	8%

Table G-2: Conversion efficiency parameters and results for the Plasma FT MD pathway. The baseline is based on the first 2900 tpd case from Motycka [40]. The cases that are demonstrated in the sensitivity analysis are the first 1200 tpd case from Juniper Consultancy [44] and the case from Minutillo et al. [37] Since there is limited data available for the Plasma FT MD pathway, the cases below are estimations to indicate the possible range of results. For example, Minutillo et al. [37] do not provide economic data and therefore, the scale and capital cost from Motycka are used [40].

		Motycka [40]		Juniper Consultancy [44], Boerrigter et al. [45]			Minutillo et al. [37], Boerrigter et al. [45]
Conversion yields and other parameters	Scale (tpd_{MSW})	2900	2900	1200	1200	1200	2900 [40]
	Jet fuel (MJ/MJ_{PMSW})	12.4%	12.0%	12.2%	8.6%	16.2%	19.6%
	Diesel (MJ/MJ_{PMSW})	16.9%	16.3%	16.6%	11.7%	22.1%	26.8%
	Gasoline (MJ/MJ_{PMSW})	9.2%	8.9%	9.0%	6.3%	12.0%	14.5%
	Net electricity (MJ/MJ_{PMSW})	8.9%	0%	9.8%	18.8%	-2.2%	-19.9%
	Total capital investment ($M)	643	643	366	366	366	643 [40]
Lifecycle GHG emissions (gCO_2e/MJ)	Median	61.74	73.59	57.21	66.04	55.12	96.84
	Mean	61.65	73.51	57.23	66.14	55.04	96.88
	Standard deviation	8.92	10.51	8.39	9.28	7.79	6.98
Minimum selling price ($/L)	Median	1.81	2.10	2.81	3.78	2.30	1.47
	Mean	1.82	2.12	2.83	3.81	2.31	1.48
	Standard deviation	0.27	0.28	0.38	0.54	0.29	0.18
Net present value ($B)	Median	-0.733	-0.910	-0.559	-0.573	-0.556	-0.840
	Mean	-0.737	-0.916	-0.564	-0.579	-0.558	-0.848
	Standard deviation	0.249	0.251	0.124	0.112	0.139	0.336
Probability of positive NPV		0.2%	0%	0%	0%	0%	58%

Table G-3: Conversion efficiency parameters and results for the ATJ MD pathway. Note that the energy balances from the cited sources are combined with the alcohol-to-jet conversion balances from Staples et al. [47] for all the cases below. The baseline is based on the second 3100 tpd case from Jones et al. [13] The cases that are demonstrated in the sensitivity analysis are the first 3100 tpd case from Jones et al. [13] and the case from Mu et al. [50] Since the latter does not provide economic data, the scale and capital cost from Jones et al. are used [13]. It should also be noted that Dutta et al. [52] modeled a direct gasification system in contrast to the indirectly-heated gasifiers modeled by Dutta et al. [51], Jones et al. [13] and Mu et al. [50] There is limited data available for the Enerkem process, the case below is an estimation based on data from a company presentation [125] and a proposal to the United States Department of Energy [126].

		Enerkem [125, 126]	Jones et al. [13]		Dutta et al. [51]	Dutta et al. [52]	Jacobs Consultancy [83]	Mu et al. [50]
Conversion yields and other parameters	Scale (tpd_{MSW})	500	3100	3100	3100	3100	4700	3100 [13]
	Jet fuel (MJ/MJ_{PMSW})	20.2%	10. 7%	15.5%	22.5%	22.3%	21.9%	25.3%
	Diesel (MJ/MJ_{PMSW})	5.5%	2.9%	4.2%	6.1%	6.1%	6.0%	6.9%
	Gasoline (MJ/MJ_{PMSW})	5.7%	3.0%	4.4%	6.4%	6.3%	6.2%	7.2%
	Higher alcohols (MJ/MJ_{PMSW})	0%	7.8%	7.4%	5.0%	7.9%	0.0%	9.0%
	Net electricity (MJ/MJ_{PMSW})	-3.5%	2.3%	0.7%	0.0%	1.0%	0.0%	0.0%
	Total capital investment ($M)	166	499	377	497	723	631	377 [13]
Lifecycle GHG emissions (gCO_2e/MJ)	Median	78.11	67.37	52.40	47.25	41.67	55.18	35.38
	Mean	78.13	67.38	52.51	47.18	41.59	55.16	35.41
	Standard deviation	13.25	15.75	12.82	9.77	9.11	11.19	8.26
Minimum selling price ($/L)	Median	4.12	2.67	1.24	1.29	2.02	1.18	0.65
	Mean	4.16	2.69	1.25	1.31	2.04	1.19	0.66
	Standard deviation	0.48	0.42	0.23	0.20	0.29	0.17	0.16
Net present value ($B)	Median	-0.329	-0.644	-0.248	-0.412	-0.906	-0.483	0.023
	Mean	-0.332	-0.652	-0.252	-0.415	-0.913	-0.487	0.023
	Standard deviation	0.053	0.163	0.158	0.218	0.263	0.307	0.205
Probability of positive NPV		0%	0%	6%	3%	0%	6%	54%

Appendix H Detailed sensitivity analysis results for MSP and NPV

The following tables list the mean, median and standard deviation measures of the minimum selling price and net present value results from the sensitivity analysis (some of the results are graphically presented in Figure 3-2 and Figure 3-3).

Table H-1: Detailed results of the MSP and NPV sensitivity analysis for the FT MD pathway

		Discount rate		Feedstock cost ($/tonne)		Income tax rate		Carbon price ($/tonne)
		3.2%	22%	-55	55	0%	39%	48.56
Minimum selling price ($/L)	Median	0.46	1.43	0.75	1.27	0.90	1.24	0.89
	Mean	0.46	1.45	0.77	1.29	0.92	1.26	0.91
	Standard deviation	0.08	0.19	0.14	0.14	0.13	0.17	0.14
Net present value ($B)	Median	0.891	-0.580	-0.049	-0.655	-0.271	-0.446	-0.211
	Mean	0.909	-0.583	-0.046	-0.658	-0.268	-0.454	-0.210
	Standard deviation	0.903	0.216	0.309	0.325	0.360	0.252	0.309
Probability of positive NPV		84%	0.4%	44%	2%	23%	4%	25%

Table H-2: Detailed results of the MSP and NPV sensitivity analysis for the Plasma FT MD pathway

		Discount rate		Feedstock cost ($/tonne)		Income tax rate		Carbon price ($/tonne)
		3.2%	22%	-55	55	0%	39%	48.56
Minimum selling price ($/L)	Median	0.72	2.64	1.41	2.24	1.63	2.25	1.72
	Mean	0.73	2.67	1.43	2.27	1.65	2.28	1.74
	Standard deviation	0.17	0.40	0.28	0.30	0.26	0.35	0.29
Net present value ($B)	Median	-0.031	-0.887	-0.468	-1.051	-0.723	-0.788	-0.682
	Mean	-0.027	-0.894	-0.473	-1.058	-0.728	-0.801	-0.691
	Standard deviation	0.625	0.199	0.242	0.264	0.269	0.224	0.252
Probability of positive NPV		48%	0%	2.5%	0%	0.3%	0%	0.3%

Table H-3: Detailed results of the MSP and NPV sensitivity analysis for the ATJ MD pathway

		Discount rate		Feedstock cost ($/tonne)		Income tax rate		Carbon price ($/tonne)
		3.2%	22%	-55	55	0%	39%	48.56
Minimum selling price ($/L)	Median	0.34	1.87	0.64	1.79	1.06	1.58	1.14
	Mean	0.35	1.90	0.66	1.81	1.08	1.61	1.16
	Standard deviation	0.16	0.36	0.24	0.30	0.25	0.32	0.27
Net present value ($B)	Median	0.461	-0.382	0.018	-0.528	-0.202	-0.304	-0.208
	Mean	0.477	-0.384	0.022	-0.532	-0.202	-0.308	-0.208
	Standard deviation	0.430	0.123	0.159	0.173	0.186	0.134	0.164
Probability of positive NPV		87%	0.1%	55%	0.1%	14%	1%	10%

Bibliography

[1] United States Environmental Protection Agency. (March 2016). *Sources of Greenhouse Gas Emissions*. Available: https://www3.epa.gov/climatechange/ghgemissions/sources/transportation.html

[2] United States Energy Information Administration. (March 2016). *Total Energy*. Available: http://www.eia.gov/totalenergy/data/monthly/index.cfm#consumption

[3] United States Energy Information Administration. (March 2016). *Annual Energy Outlook 2015*. Available: http://www.eia.gov/oiaf/aeo/tablebrowser/

[4] United States Environmental Protection Agency. (March 2016). *Renewable Fuel Standard Program*. Available: http://www.epa.gov/otaq/fuels/renewablefuels/index.htm

[5] United States Federal Aviation Administration. (March 2016). *Destination 2025*. Available: https://www.faa.gov/about/plans_reports/media/Destination2025.pdf

[6] United States Environmental Protection Agency, "Advancing Sustainable Materials Management: Facts and Figures 2013," EPA530-R-15-002, 2015.

[7] United States Environmental Protection Agency. (March 2016). *Overview of Greenhouse Gases*. Available: https://www3.epa.gov/climatechange/ghgemissions/gases/ch4.html

[8] G. Seber, R. Malina, M. N. Pearlson, H. Olcay, J. I. Hileman, and S. R. H. Barrett, "Environmental and economic assessment of producing hydroprocessed jet and diesel fuel from waste oils and tallow," *Biomass and Bioenergy*, vol. 67, pp. 108-118, 2014.

[9] C. Valkenburg, M. A. Gerber, C. W. Walton, S. B. Jones, B. L. Thompson, and D. J. Stevens, "Municipal Solid Waste (MSW) to Liquid Fuels Synthesis, Volume 1: Availability of Feedstock and Technology," Pacific Northwest National Laboratory PNNL-18144, 2008.

[10] P. N. Pressley, T. N. Aziz, J. F. DeCarolis, M. A. Barlaz, F. He, F. Li, *et al.*, "Municipal solid waste conversion to transportation fuels: a life-cycle estimation of global warming potential and energy consumption," *Journal of Cleaner Production*, vol. 70, pp. 145-153, 2014.

[11] A. M. Niziolek, O. Onel, M. M. F. Hasan, and C. A. Floudas, "Municipal solid waste to liquid transportation fuels – Part II: Process synthesis and global optimization strategies," *Computers & Chemical Engineering*, vol. 74, pp. 184-203, 2015.

[12] A. K. Epstein, K. C. Lewis, M. Epstein, R. Hernandez, S. Kramer, M. Lakeman, *et al.*, "Developing efficient and cost-effective use of wastes as feedstocks," Commercial Aviation Alternative Fuels Initiative, 2013.

[13] S. B. Jones, Y. Zhu, and C. Valkenburg, "Municipal Solid Waste (MSW) to Liquid Fuels Synthesis, Volume 2: A Techno-economic Evaluation of the Production of Mixed Alcohols," Pacific Northwest National Laboratory PNNL-18482, 2009.

[14] A. U. Zaman, "Comparative study of municipal solid waste treatment technologies using life cycle assessment method," *International Journal of Environmental Science & Technology,* vol. 7, pp. 225-234, 2010.

[15] H. Stichnothe and A. Azapagic, "Bioethanol from waste: Life cycle estimation of the greenhouse gas saving potential," *Resources, Conservation and Recycling,* vol. 53, pp. 624-630, 2009.

[16] F. C. Luz, M. H. Rocha, E. E. S. Lora, O. J. Venturini, R. V. Andrade, M. M. V. Leme, *et al.*, "Techno-economic analysis of municipal solid waste gasification for electricity generation in Brazil," *Energy Conversion and Management,* vol. 103, pp. 321-337, 2015.

[17] M. M. V. Leme, M. H. Rocha, E. E. S. Lora, O. J. Venturini, B. M. Lopes, and C. H. Ferreira, "Techno-economic analysis and environmental impact assessment of energy recovery from Municipal Solid Waste (MSW) in Brazil," *Resources, Conservation and Recycling,* vol. 87, pp. 8-20, 2014.

[18] H. H. Khoo, "Life cycle impact assessment of various waste conversion technologies," *Waste Management,* vol. 29, pp. 1892-1900, 2009.

[19] R. M. Swanson, J. A. Satrio, R. C. Brown, A. Platon, and D. D. Hsu, "Techno-Economic Analysis of Biofuels Production Based on Gasification," National Renewable Energy Laboratory NREL/TP-6A20-46587, 2010.

[20] T. G. Kreutz, E. D. Larson, G. Liu, and R. H. Williams, "Fischer-Tropsch Fuels from Coal and Biomass," presented at the 25th Annual International Pittsburgh Coal Conference, Pittsburgh, Pennsylvania, USA, 2008.

[21] E. D. Larson, H. Jin, and F. E. Celik, "Large-scale gasification-based coproduction of fuels and electricity from switchgrass," *Biofuels, Bioproducts and Biorefining,* vol. 3, pp. 174-194, 2009.

[22] X. Xie, M. Wang, and J. Han, "Assessment of fuel-cycle energy use and greenhouse gas emissions for Fischer-Tropsch diesel from coal and cellulosic biomass," *Environmental Science and Technology,* vol. 45, pp. 3047-3053, 2011.

[23] C. N. Hamelinck, A. P. C. Faaij, H. den Uil, and H. Boerrigter, "Production of FT transportation fuels from biomass; technical options, process analysis and optimisation, and development potential," *Energy*, vol. 29, pp. 1743-1771, 2004.

[24] Y. Zhu, S. A. Tjokro Rahardjo, C. Valkenburg, L. J. Snowden-Swan, S. B. Jones, and M. A. Machinal, "Techno-economic Analysis for the Thermochemical Conversion of Biomass to Liquid Fuels," Pacific Northwest National Laboratory PNNL-19009, 2011.

[25] M. Siedlecki, W. De Jong, and A. H. M. Verkooijen, "Fluidized Bed Gasification as a Mature And Reliable Technology for the Production of Bio-Syngas and Applied in the Production of Liquid Transportation Fuels—A Review," *Energies*, vol. 4, pp. 389-434, 2011.

[26] O. P. R. van Vliet, A. P. C. Faaij, and W. C. Turkenburg, "Fischer–Tropsch diesel production in a well-to-wheel perspective: A carbon, energy flow and cost analysis," *Energy Conversion and Management*, vol. 50, pp. 855-876, 2009.

[27] D. Unruh, K. Pabst, and G. Schaub, "Fischer−Tropsch Synfuels from Biomass: Maximizing Carbon Efficiency and Hydrocarbon Yield," *Energy & Fuels*, vol. 24, pp. 2634-2641, 2010.

[28] United States Environmental Protection Agency. (September 2015). *Waste Reduction Model (WARM) Version 13 (updated March 2015)*. Available: https://www.epa.gov/warm

[29] Argonne National Laboratory. (November 2015). *The Greenhouse Gases, Regulated Emissions, and Energy Use in Transportation Model (GREET.net) 2015 Release*. Available: https://greet.es.anl.gov

[30] M. Chester and E. Martin, "Cellulosic Ethanol from Municipal Solid Waste: A Case Study of the Economic, Energy, and Greenhouse Gas Impacts in California," *Environmental Science & Technology*, vol. 43, pp. 5183-5189, 2009.

[31] J. Ebner, C. Babbitt, M. Winer, B. Hilton, and A. Williamson, "Life cycle greenhouse gas (GHG) impacts of a novel process for converting food waste to ethanol and co-products," *Applied Energy*, vol. 130, pp. 86-93, 2014.

[32] D. Hoornweg and P. Bhada-Tata, "What a Waste - A Global Review of Solid Waste Management," The World Bank, 2012.

[33] V. Choudhry and S. R. Hadley, "Utilization of Coal Gasification Slag," in *Clean Energy from Waste and Coal*. vol. 515, American Chemical Society, 1992, pp. 253-263.

[34] A. Steynberg and M. Dry, *Fischer-Tropsch technology*. Amsterdam ; Boston: Elsevier, 2004.

[35] B. Lemmens, H. Elslander, I. Vanderreydt, K. Peys, L. Diels, M. Oosterlinck, *et al.*, "Assessment of plasma gasification of high caloric waste streams," *Waste Management,* vol. 27, pp. 1562-1569, 2007.

[36] K. Moustakas, D. Fatta, S. Malamis, K. Haralambous, and M. Loizidou, "Demonstration plasma gasification/vitrification system for effective hazardous waste treatment," *Journal of Hazardous Materials,* vol. 123, pp. 120-126, 2005.

[37] M. Minutillo, A. Perna, and D. Di Bona, "Modelling and performance analysis of an integrated plasma gasification combined cycle (IPGCC) power plant," *Energy Conversion and Management,* vol. 50, pp. 2837-2842, 2009.

[38] J. G. Speight, "Production of syngas, synfuel, bio-oils, and biogas from coal, biomass, and opportunity fuels " in *Fuel Flexible Energy Generation*, J. Oakey, Ed., Boston: Woodhead Publishing, 2016, pp. 145-174.

[39] S. Lee and Y. T. Shah, *Biofuels and bioenergy : processes and technologies*. Boca Raton, FL: Taylor & Francis, 2012.

[40] S. A. Motycka, "Techno Economic Analysis Of A Plasma Gasification Biomass To Liquids Plant " Doctor of Philosophy thesis, School of Engineering and Applied Sciences, George Washington University, 2013.

[41] A. N. Bratsev, V. E. Popov, A. F. Rutberg, and S. V. Shtengel', "A facility for plasma gasification of waste of various types," *High Temperature,* vol. 44, pp. 823-828, 2006.

[42] Q. Zhang, L. Dor, D. Fenigshtein, W. Yang, and W. Blasiak, "Gasification of municipal solid waste in the Plasma Gasification Melting process," *Applied Energy,* vol. 90, pp. 106-112, 2012.

[43] A. Mountouris, E. Voutsas, and D. Tassios, "Solid waste plasma gasification: Equilibrium model development and exergy analysis," *Energy Conversion and Management,* vol. 47, pp. 1723-1737, 2006.

[44] Juniper Consultancy Services Limited, "The Alter NRG/Westinghouse Plasma Gasification Process," 2008.

[45] H. Boerrigter, H. d. Uil, and H.-P. Calis, "Green Diesel from Biomass via Fischer-Tropsch synthesis: New Insights in Gas Cleaning and Process Design," presented at the Pyrolysis and Gasification of Biomass and Waste, Expert Meeting, Strasbourg, France, 2002.

[46] J. L. Manganaro, B. Chen, J. Adeosun, S. Lakhapatri, D. Favetta, A. Lawal, *et al.*, "Conversion of Waste Biomass into Liquid Transportation Fuel: An Energy Analysis," *Energy & Fuels,* vol. 25, pp. 2711-2720, 2011.

[47] M. D. Staples, R. Malina, H. Olcay, M. N. Pearlson, J. I. Hileman, A. Boies, *et al.*, "Lifecycle greenhouse gas footprint and minimum selling price of renewable diesel and jet fuel from fermentation and advanced fermentation production technologies," *Energy & Environmental Science,* vol. 7, p. 1545, 2014.

[48] Enerkem Alberta Biofuels LP. (March 2016). *Enerkem Alberta Biofuels: a global game-changing facility*. Available: http://enerkem.com/facilities/enerkem-alberta-biofuels/

[49] S. C. Marie-Rose, A. L. Perinet, and J.-M. Lavoie, "Conversion of Non-Homogeneous Biomass to Ultraclean Syngas and Catalytic Conversion to Ethanol," in *Biofuel's Engineering Process Technology*, Marco Aurelio Dos Santos Bernardes, Ed., InTech, 2011.

[50] D. Mu, T. Seager, P. S. Rao, and F. Zhao, "Comparative life cycle assessment of lignocellulosic ethanol production: Biochemical versus thermochemical conversion," *Environmental Management,* vol. 46, pp. 565-578, 2010.

[51] A. Dutta, M. Talmadge, J. Hensley, M. Worley, D. Dudgeon, D. Barton, *et al.*, "Techno-economics for conversion of lignocellulosic biomass to ethanol by indirect gasification and mixed alcohol synthesis," *Environmental Progress & Sustainable Energy,* vol. 31, pp. 182-190, 2012.

[52] A. Dutta and S. D. Phillips, "Thermochemical Ethanol via Direct Gasification and Mixed Alcohol Synthesis of Lignocellulosic Biomass," National Renewable Energy Laboratory NREL/TP-510-45913, 2009.

[53] S. Phillips, A. Aden, J. Jechura, D. Dayton, and T. Eggeman, "Thermochemical Ethanol via Direct Gasification and Mixed Alcohol Synthesis of Lignocellulosic Biomass," National Renewable Energy Laboratory NREL/TP-510-41168, 2007.

[54] P. Forster, V. Ramaswamy, P. Artaxo, T. Berntsen, R. Betts, D. W. Fahey, *et al.*, "Changes in Atmospheric Constituents and in Radiative Forcing," in *Climate Change 2007: The Physical Science Basis. Contribution of Working Group I to the Fourth Assessment Report of the Intergovernmental Panel on Climate Change*, S. Solomon, D. Qin, M. Manning, Z. Chen, M. Marquis, K. B. Averyt, *et al.*, Eds., Cambridge, United Kingdom and New York, NY, USA: Cambridge University Press, 2007.

[55] M. Wang, H. Huo, and S. Arora, "Methods of dealing with co-products of biofuels in life-cycle analysis and consequent results within the U.S. context," *Energy Policy,* vol. 39, pp. 5726-5736, 2011.

[56] Intergovernmental Panel on Climate Change, *2006 IPCC Guidelines for National Greenhouse Gas Inventories, Prepared by the National Greenhouse Gas Inventories Programme* vol. 2. Japan: IGES, 2006.

[57] United States Energy Information Administration, "Methodology for Allocating Municipal Solid Waste to Biogenic and Non-Biogenic Energy," 2007.

[58] United States Environmental Protection Agency. (September 2015). *"Combustion" in Documentation for Greenhouse Gas Emission and Energy Factors Used in the Waste Reduction Model (WARM) Version 13*. Available: https://www3.epa.gov/warm/pdfs/WARM_Documentation.pdf

[59] R. B. Williams, B. M. Jenkins, and D. Nguyen, "Solid Waste Conversion: A review and database of current and emerging technologies," California Integrated Waste Management Board IWM-C0172, 2003.

[60] B. M. Guell, M. Bugge, R. S. Kempegowda, A. George, and S. M. Paap, "Benchmark of conversion and production technologies for synthetic biofuels for aviation," SINTEF Energy Research, 2012.

[61] G. Doka, "Life Cycle Inventories of Waste Treatment Services, ecoinvent report No. 13," Swiss Centre for Life Cycle Inventories, Dübendorf, 2003.

[62] F. Cherubini, S. Bargigli, and S. Ulgiati, "Life cycle assessment (LCA) of waste management strategies: Landfilling, sorting plant and incineration," *Energy,* vol. 34, pp. 2116-2123, 2009.

[63] R. Chandrappa and D. B. Das, "Waste Quantities and Characteristics," in *Solid Waste Management: Principles and Practice*, Springer-Verlag Berlin Heidelberg, 2012, pp. 47-63.

[64] G. Tchobanoglous, H. Theisen, and S. A. Vigil, *Integrated solid waste management: engineering principles and management issues*: McGraw-Hill, 1993.

[65] Intergovernmental Panel on Climate Change, *Good Practice Guidance and Uncertainty Management in National Greenhouse Gas Inventories*. Hayama, Japan: IPCC/OECD/IEA/IGES, 2000.

[66] United States Environmental Protection Agency. (January 2016). *Emissions & Generation Resource Integrated Database (eGRID) 2012 Data File*. Available: https://www.epa.gov/energy/egrid

[67] P. N. Pressley, J. W. Levis, A. Damgaard, M. A. Barlaz, and J. F. DeCarolis, "Analysis of material recovery facilities for use in life-cycle assessment," *Waste Management,* vol. 35, pp. 307-317, 2015.

[68] A. C. Caputo and P. M. Pelagagge, "RDF production plants: I. Design and costs," *Applied Thermal Engineering*, vol. 22, pp. 423-437, 2002.

[69] United States Energy Information Administration. (January 2016). *Refiner Petroleum Product Prices by Sales Type*. Available: https://www.eia.gov/dnav/pet/pet_pri_refoth_dcu_nus_a.htm

[70] D. Ramey and S.-T. Yang, "Production of Butyric Acid and Butanol from Biomass," United States Department of Energy, 2004.

[71] R. Brown, "Propanol Prices Experience Upward Pressure," *Chemical Market Reporter*, vol. 263, p. 14, 2003.

[72] Bloomberg L.P. (January 2016). *Historical Price Line Chart for ACFFPCDT, Average Cost of Fossil Fuels Pet Coke Dollars per Ton - US DOE source, 2006 - 2015*.

[73] United States Geological Survey, "Mineral Commodity Summaries 2016," United States Geological Survey, 2016.

[74] Metalprices.com. (January 2016). *Aluminum Cans (UBC)*. Available: https://www.metalprices.com/metal/aluminum/aluminum-cans-ubc

[75] S. Nishtala and E. Solano-Mora. (January 2016). *Description of the Material Recovery Facilities Process Model Design, Cost, and Life-Cycle Inventory for the MSW-DST Tool, Research Triangle Institute*. Available: https://mswdst.rti.org/resources.htm

[76] Southern Resources. (January 2016). *Scrap Prices*. Available: http://www.southernresources.com/compare-prices

[77] Scrap Register Prices. (January 2016). *United States Scrap Metal Prices*. Available: http://www.scrapregister.com/scrap-price/united-states/260

[78] Kessler Consulting Inc., "Materials recovery facility feasibility study," Pinellas County Department of Solid Waste Operations, 2009.

[79] M. Pearlson, C. Wollersheim, and J. Hileman, "A techno-economic review of hydroprocessed renewable esters and fatty acids for jet fuel production," *Biofuels, Bioproducts and Biorefining*, vol. 7, pp. 89-96, 2013.

[80] Organisation for Economic Co-operation and Development (OECD), "Industrial Water Pricing in OECD Countries," ENV/EPOC/GEEI(98)10/FINAL, 1999.

[81] N.-B. Chang and S. F. Wang, "The development of material recovery facilities in the United States: status and cost structure analysis," *Resources, Conservation and Recycling*, vol. 13, pp. 115-128, 1995.

[82] B. A. Hegberg, W. H. Hallenbeck, G. R. Brenniman, and R. A. Wadden, "Municipal solid waste incineration with energy recovery in the U.S.A. - Technologies, facilities and

vendors for less than 550 tons per day " *Waste Management & Research*, vol. 9, pp. 127-152, 1991.

[83] Jacobs Consultancy, "Final Report: Identification of Opportunities for the Production of Bio-Products from Waste Bio-Mass in Alberta," University of Alberta, Calgary, 2013.

[84] A. L. Bozec, "Costs models for each municipal solid waste process, Aid in the Management and European Comparison of Municipal Solid Waste Treatment methods for a Global and Sustainable Approach," European Commission, 2004.

[85] A. J. Dubanowitz, "Design of a Materials Recovery Facility (MRF) For Processing the Recyclable Materials of New York City's Municipal Solid Waste," Master of Science thesis, Department of Earth and Environmental Engineering, Columbia University, 2000.

[86] Resource Recycling Systems and StewardEdge Inc., "Volume 3: Cost Modelling, A Study of the Optimization of the Blue Box Material Processing System in Ontario," Waste Diversion Ontario, 2012.

[87] SRI International, "Data Summary of Municipal Solid Waste Management Alternatives," National Renewable Energy Laboratory NREL/TP-431-4988D, 1992.

[88] J. H. Gary, G. E. Handwerk, and M. J. Kaiser, *Petroleum Refining: Technology and Economics*, 5 ed., Basel, Switzerland: Taylor & Francis, 2007.

[89] United States Environmental Protection Agency. (September 2015). *"Landfilling" in Documentation for Greenhouse Gas Emission and Energy Factors Used in the Waste Reduction Model (WARM) Version 13*. Available: https://www3.epa.gov/warm/pdfs/WARM_Documentation.pdf

[90] United States Environmental Protection Agency. (September 2015). *"Recycling" in Documentation for Greenhouse Gas Emission and Energy Factors Used in the Waste Reduction Model (WARM) Version 13*. Available: https://www3.epa.gov/warm/pdfs/WARM_Documentation.pdf

[91] X. Zhao, T. R. Brown, and W. E. Tyner, "Stochastic techno-economic evaluation of cellulosic biofuel pathways," *Bioresource Technology*, vol. 198, pp. 755-763, 2015.

[92] D. Blazy, M. N. Pearlson, B. Miller, and R. E. Bartlett, "A Monte Carlo-based Methodology for Valuing Refineries Producing Aviation Biofuel," in *Commercializing Biobased Products : Opportunities, Challenges, Benefits, and Risks*, S. W. Snyder, Ed., The Royal Society of Chemistry, 2016, pp. 336-351.

[93] United States Government Accountability Office, "Corporate Income Tax: Effective Tax Rates Can Differ Significantly from the Statutory Rate," GAO-13-520, 2013.

[94] Fulcrum BioEnergy. (March 2016). *Fulcrum BioEnergy proves trash-to-jet fuel method, gets DOD grant*. Available: http://biomassmagazine.com/articles/9039/fulcrum-bioenergy-proves-trash-to-jet-fuel-method-gets-dod-grant#

[95] A. C. Caputo and P. M. Pelagagge, "RDF production plants: II. Economics and profitability," *Applied Thermal Engineering*, vol. 22, pp. 439-448, 2002.

[96] Economic indicators, *Chemical Engineering*, vol. 123, p. 68, 2016.

[97] United States Energy Information Administration. (January 2016). *United States Natural Gas Industrial Price*. Available: http://www.eia.gov/dnav/ng/hist/n3035us3A.htm

[98] United States Energy Information Administration. (January 2016). *Average retail price of electricity*. Available: http://www.eia.gov/electricity/data/browser/#/topic/7?agg=2,0,1&geo=g&freq=M&start=200101&end=201505&ctype=linechart&ltype=pin&rtype=s

[99] United States Bureau of Labor Statistics. (January 2016). *Database for Inflation & Prices*. Available: http://www.bls.gov/data/#prices

[100] United States Bureau of Labor Statistics. (January 2016). *Database for Pay & Benefits*. Available: http://www.bls.gov/data/#wages

[101] M. A. Stephens, "EDF Statistics for Goodness of Fit and Some Comparisons," *Journal of the American Statistical Association*, vol. 69, pp. 730-737, 1974.

[102] A. Bittner, W. E. Tyner, and X. Zhao, "Field to flight: A techno-economic analysis of the corn stover to aviation biofuels supply chain," *Biofuels, Bioproducts and Biorefining*, vol. 9, pp. 201-210, 2015.

[103] R. Petter and W. E. Tyner, "Technoeconomic and policy analysis for corn stover biofuels," *ISRN Economics*, vol. 2014, 2014.

[104] Y. Zhu, M. J. Biddy, S. B. Jones, D. C. Elliott, and A. J. Schmidt, "Techno-economic analysis of liquid fuel production from woody biomass via hydrothermal liquefaction (HTL) and upgrading," *Applied Energy*, vol. 129, pp. 384-394, 2014.

[105] B. Li, L. Ou, Q. Dang, P. Meyer, S. Jones, R. Brown, *et al.*, "Techno-economic and uncertainty analysis of in situ and ex situ fast pyrolysis for biofuel production," *Bioresource Technology*, vol. 196, pp. 49-56, 2015.

[106] S. Höltinger, J. Schmidt, M. Schönhart, and E. Schmid, "A spatially explicit techno-economic assessment of green biorefinery concepts," *Biofuels, Bioproducts and Biorefining*, vol. 8, pp. 325-341, 2014.

[107] T. R. Brown, "A critical analysis of thermochemical cellulosic biorefinery capital cost estimates," *Biofuels, Bioproducts and Biorefining,* vol. 9, pp. 412-421, 2015.

[108] R. W. Stratton, H. M. Wong, and J. I. Hileman, "Quantifying Variability in Life Cycle Greenhouse Gas Inventories of Alternative Middle Distillate Transportation Fuels," *Environmental Science & Technology,* vol. 45, pp. 4637-4644, 2011.

[109] MathWorks. (March 2016). *R2016a Documentation: 'ksdensity', Kernel smoothing function estimate for univariate and bivariate data*. Available: http://www.mathworks.com/help/stats/ksdensity.html

[110] D. Offenhuber, D. Lee, M. I. Wolf, S. Phithakkitnukoon, A. Biderman, and C. Ratti, "Putting Matter in Place," *Journal of the American Planning Association,* vol. 78, pp. 173-196, 2012.

[111] United States Office of Management and Budget. (March 2016). *Circular A-94 Appendix C, Revised November 2015, Discount rates for cost-effectiveness, lease purchase, and related analyses*. Available: https://www.whitehouse.gov/omb/circulars_a094/a94_appx-c

[112] Organisation for Economic Co-operation and Development (OECD). (March 2016). *Tax database, Table II.1. Corporate income tax rate*. Available: http://stats.oecd.org//Index.aspx?QueryId=58204

[113] United States Government Interagency Working Group on Social Cost of Carbon, "Technical Support Document: -Technical Update of the Social Cost of Carbon for Regulatory Impact Analysis - Under Executive Order 12866," 2013 (revised July 2015).

[114] N. J. Themelis and C. Mussche, "Municipal solid waste management and waste-to-energy in the United States, China and Japan " presented at the 2nd International Academic Symposium on Enhanced Landfill Mining, Houthalen-Helchteren, 2013.

[115] R. W. Stratton, P. J. Wolfe, and J. I. Hileman, "Impact of Aviation Non-CO2 Combustion Effects on the Environmental Feasibility of Alternative Jet Fuels," *Environmental Science & Technology,* vol. 45, pp. 10736-10743, 2011.

[116] J. Morris, "Bury or burn North America MSW? LCAs provide answers for climate impacts & carbon neutral power potential," *Environmental Science & Technology,* vol. 44, pp. 7944-9, 2010.

[117] Y. Kalogo, S. Habibi, H. L. MacLean, and S. V. Joshi, "Environmental Implications of Municipal Solid Waste-Derived Ethanol," *Environmental Science & Technology,* vol. 41, pp. 35-41, 2007.

[118] M. M. Wright, D. E. Daugaard, J. A. Satrio, and R. C. Brown, "Techno-economic analysis of biomass fast pyrolysis to transportation fuels," *Fuel,* vol. 89, pp. S2-S10, 2010.

[119] MathWorks. (March 2016). *R2016a Documentation: 'histogram', Histogram plot*. Available: http://www.mathworks.com/help/matlab/ref/histogram.html

[120] MathWorks. (March 2016). *R2016a Documentation: 'skewness', Skewness*. Available: http://www.mathworks.com/help/stats/skewness.html

[121] MathWorks. (March 2016). *R2016a Documentation: 'kurtosis', Kurtosis*. Available: http://www.mathworks.com/help/stats/kurtosis.html

[122] M. G. Bulmer, *Principles of Statistics*. New York: Dover 1979.

[123] L. T. DeCarlo, "On the Meaning and Use of Kurtosis," *Psychological Methods,* vol. 2, pp. 292-307, 1997.

[124] K. P. Balanda and H. L. MacGillivray, "Kurtosis: A critical review," *American Statistician,* vol. 42, pp. 111-119, 1988.

[125] E. Chornet. (September 2015). *Valorizing Residual Carbon: An Important Link Between Energy and the Environment*. Available: http://www.ai-ees.ca/wp-content/uploads/2016/03/2012-rer-esteban_chornet-valorizing_residual_carbon.pdf

[126] Enerkem Corporation, "Construction and Operation of a Heterogeneous Feed Biorefinery," United States Department of Energy DOE/EA-1790, 2010.